PREPARATION AND CHARACTERIZATION OF CALCITE ($CaCO_3$) PARTICULATE FILLED THERMOPLASTIC COMPOSITES

A Thesis Submitted to
the Graduate School of Engineering and Sciences of
İzmir Institute of Technology
in Partial Fulfillment of the Requirements for the Degree of

MASTER OF SCIENCE

in Mechanical Engineering

by
Esin KIZILTEPE

July 2014
İZMİR

We approve the thesis of **Esin KIZILTEPE**

Examining Committee Members:

_____

Prof. Dr. Metin TANOĞLU
Department of Mechanical Engineering, İzmir Institute of Technology

_____

Assoc. Prof. Dr. Ekrem ÖZDEMİR
Department of Chemical Engineering, İzmir Institute of Technology

_____

Dr. Sinan KANDEMİR
Department of Mechanical Engineering, İzmir Institute of Technology

11 July 2014

_____

Prof. Dr. Metin TANOĞLU
Supervisor, Department of Mechanical Engineering
İzmir Institute of Technology

_____

Prof. Dr. Metin TANOĞLU
Head of the Department of
Mechanical Engineering

_____

Prof. Dr. R. Tuğrul SENGER
Dean of the Graduate School of
Engineering and Sciences

ACKNOWLEDGMENTS

I would like to express my deepest gratitude to my thesis supervisor Prof. Dr. Metin TANOĞLU for his guidance, understanding, kind support and encouraging advices throughout my thesis.

I am especially grateful to Bertan BEYLERGİL for his support and assistance to my work.

I would like to thank to my laboratory colleagues, Serkan KANGAL, Mehmet Deniz GÜNEŞ, Oylum ÇOLPANKAN for their helps and supports.

Lastly, I would like to thank to my dear family for their endless encouragement and support during my master thesis study.

ABSTRACT

PREPARATION AND CHARACTERIZATION OF CALCITE ($CaCO_3$) PARTICULATE FILLED THERMOPLASTIC COMPOSITES

Nano-sized particle filled polymer composites have been received great attention of researchers and industrial institutions in recent years due to their unique properties, save as high mechanical strength, thermal and solvent resistance as compared to traditional composite materials.

In this study, calcium carbonate ($CaCO_3$) filled polypropylene (PP) and Polyethylene (PE) composite blends were prepared using a co-rotational twin screw extruder with a calcite particle content varying from 0 to 30 wt. % . Tensile and three-point bending test coupons were prepared by injection moulding using the extruded composite blends. The effects of calcite reinforcement (with and without stearic acid treatment) on the microstructural, thermal and mechanical properties of neat PP and PE were investigated. Nano-$CaCO_3$ powders were characterized by means of Scanning Electron Microscopy (SEM) and X-Ray Diffraction (XRD). The PE and PP were characterized via differential scanning calorimetry (DSC) and thermogravimetric analysis (TGA). Analytical results were compared with the experimental results.

ÖZET

KALSİT ($CaCO_3$) PARTİKÜL DOLGULU TERMOPLASTİK KOMPOZİTLERİN KARAKTERİZASYONU VE HAZIRLANMASI

Nano partikül dolgulu polimer kompozitler, yüksek mukavemet, sıcaklık ve çözücülere karşı dayanıklı olmaları gibi özellikleri nedeniyle son yıllarda, araştırmacıların ve endüstriyel kuruluşların dikkatini çekmektedir.

Bu çalışmada, ağırlıkça farklı yüzdelerde (%0-30) kalsit ($CaCO_3$) dolgulu polipropilen (PP) ve polietilen (PE) matrisli kompozitler çift vidalı ekstruder kullanılarak üretilmiştir. Test numuneleri, enjeksiyon kalıplama yöntemiyle üretilmiştir. Nano-kalsit tozlar SEM ve XRD yöntemleri ile karakterize edilmiştir. PP ve PE'nin DSC ve TGA ile termal karakterizyonu yapılmıştır. Üretilen kompozitlerin morfolojik, termal, mekanik ve darbe dayanımı özellikleri standartlara göre belirlenmiştir. Analitik sonuçlar, deneysel verilerle kıyaslanmıştır.

TABLES OF CONTENTS

LIST OF FIGURES

LIST OF TABLES

Table **Page**

CHAPTER 1

BACKGROUND INFORMATION

1.1. Introduction

A composite material is a macroscopic combination of two or more distinct phases that are insoluble in each other. At least one phase is mostly inorganic as dispersed phase. Composites have some advantages such as increased stiffness, strength, toughness, impact strength, fatigue life, mechanical damping, modified electrical properties compared to traditional materials such as steel and aluminum [1].

Composites generally consist of two phases: reinforcement phase and matrix phase. Figure 1.1 shows the phases of a composite for different types of fillers. The first constituent generally improves the mechanical properties of the matrix. It is dispersed in matrix and properties of a composite depends on properties of the constituents such as the content and geometry of the reinforcement (i.e., size and shape of the reinforcing component). Reinforcing agents are filler materials which can be minerals, metallic powders, organic by products or synthetic inorganic compounds. They can also classified according to their geometry as; particles, fibers, and flakes which may have different properties. The second constituent, matrix, is the main constituent binding the other components together in the composite. It can be metallic, ceramic or polymeric. Polymeric composites which will be interest of in this study can be divided into two main categories: (i) thermoplastic-based composites and (ii) thermoset-based composites [2].

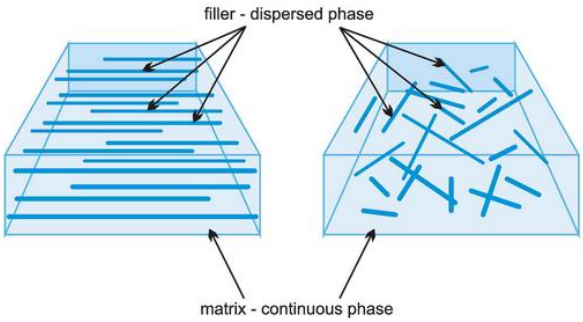

Figure 1.1. Illustrating the phases of a composite [3]

1.2. Thermoplastics

Thermoplastics have the simplest molecular structure, with chemically independent macromolecules. By heating, they are softened or melted, then shaped, formed, welded, and solidified when cooled. Multiple cycles of heating and cooling can be repeated without severe damage, allowing reprocessing and recycling [4].

There are some differences between thermoplastics and thermosetting matrices. Thermoplastics often have higher tensile strength and moduli compared to many thermosets. This is because glass transition temperature (T_g) of thermoplastic which is close to or below room temperature. In contrast, thermoplastics show high strain rates until failure. Achieving good interfacial adhesion in thermoplastic composites is a challenging task. High melt viscosities and the lack of reactive groups make them difficult to wet and bond to reinforcing fibers. The most common thermoplastic matrices are polyolefinic (polyethylene, polypropylene), vinylic polymers (polyvinyl chloride, polyamides) [5] .

1.2.1. Polyethylene

Polyethylene (PE), a member of polyolefins, has the simplest structure among all over polymers. Due to its high toughness, ductility, excellent chemical resistance, low water vapor permeability, and very low water absorption, PE is an attractive choice for a variety of applications (Figure 1.2) [6,7].

Figure 1.2. Polyethylene classification and applications [8]

1.2.2. Polypropylene

Polypropylene (PP) is another common polyolefin. Some advantages of PP are high melting point (relative to most volume plastics), good stiffness/toughness balance, excellent dielectric properties and low cost. PP is being used in the automotive industry for the production of bumpers, heater housings, door pockets and trimmings, timing belt covers cladding [10]. Figure 1.3 shows light weight polypropylene automotive parts.

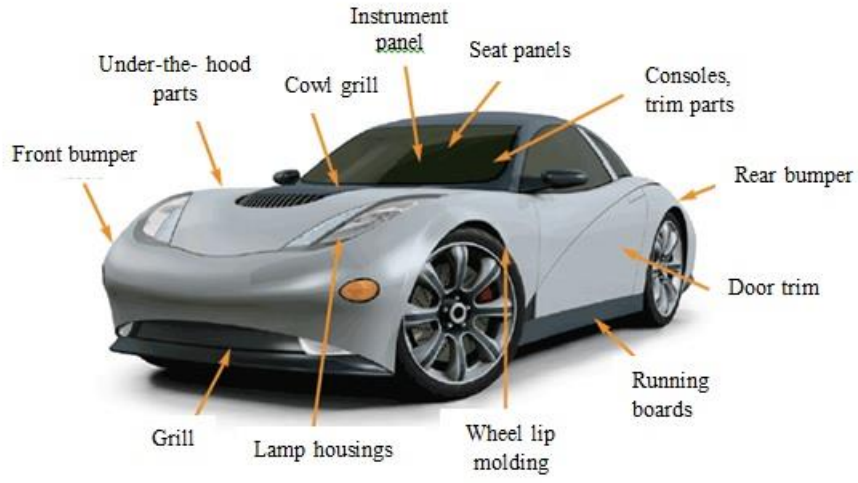

Figure 1.3. Light weight polypropylene automotive parts [11]

However, there are some disadvantages of polypropylene such as high flammability, low temperature brittleness, moderate stiffness, low UV resistance, low melt strength. Selected, typical properties for polypropylene are shown in Table 1.1.

Table 1.1. Properties of polypropylene [9]

Property	
Density, [g/cm^3]	0.90-1.24
Ultimate tensile strength, [MPa]	19.7-80.0
Tensile Modulus, [MPa]	0.5-7.6
Elongation to failure, [%]	3-887
Notched Izod at room temperature, [J/m^2]	0.16-no break
Water absorption over 24 hours, [%]	0.01-0.1
Chemical resistance	
Weak acid	Excellent
Strong acid	Varies with acid
Weak alkali	Excellent
Strong alkali	Good
Solvents	Nonpolar swells,polar
Alcohols	Excellent
T_m , [^{o}C]	130-168
T_g , [^{o}C]	-20
Processing temperature, [^{o}C]	202-252

1.3. Mineral Fillers

PP and PE are often transformed into composites by the addition of mineral fillers. According to ASTM D1566-95a [12], the term of "*filler*" is described as "*A solid compounding material, usually in a finely divided form, which may be added in relatively large proportions to a polymer for technical or economic reasons*". As mentioned before, mineral fillers are often compounded into thermoplastics to improve thermal, mechanical, and electrical properties, but also to reduce product cost. Table 1.2 shows some thermoplastic material costs.

There were three stages in the development of reinforcing composites with additional fillers. The first one started in late 1950s and was related to the development

of solid rocket fuel which contained about 80% of rigid powder particles bonded by an elastic rubber matrix. The second stage began in 1970s with the development of composites based on thermoplastic polymers filled with rigid nonorganic particles. The last stage started in late 1980s with the development of nanocomposites [13] .

Table 1.2. Order of magnitude of some thermoplastic material costs (€/lt) [14]

Thermoplastics	**Minimum**	**Maximum**
PE, PVC, PS, PP	0.8	4
ABS, SAN, SMA	3	5
PMMA, PC, PA, POM, PET, PBT, PPE	3	8
Speciality PA	7	12
PPS, PSU	7	30
PEI, PAI	20	40
PTFE	25	50
PEEK , LCP	20	120
ETFE, ECTFE, FEP, PEA	60	220

The effects of inorganic fillers on the mechanical and physical properties of the thermoplastic composites strongly depend on the filler size, shape, aspect ratio, interfacial adhesion, surface characteristics, and degree of dispersion. Table 1.3 shows the most commonly used fillers for PP.

Table 1.3. Inorganic fillers for PP compounds [15]

Oxide	Silica,Titanium oxide,Magnesium oxide
Hydroxide	Alminum hydroxide,Magnesium hydroxide,Calcium hydroxide
Carbonate	Calcium carbonate,Dolomite
Sulfate	Basic magnesium sulfate
Silicate	Talc, Clay, Mica, Glass fiber, Glass balloon, Glass beads, Calcium silicate, Montmorillonite, Bentonite
Carbon	Carbon black,Graphite,Carbon fiber

1.3.1. Calcium Carbonate ($CaCO_3$)

Calcium carbonate ($CaCO_3$) is one of the most commonly used inorganic filler. It is abundant, largely inert, low cost, white filler. Commercial $CaCO_3$ fillers are available with a range of micro to nano sizes. The main function of calcium carbonate is to lower costs, while having moderate effects on mechanical properties. The mechanical properties of polymer composites with $CaCO_3$ depend on interfaces where the polymer matrix and filler are in contact. $CaCO_3$ particles have mostly polar, hydrophilic and high free energy surfaces [16]. Therefore, these particles may not be suitable for polymer matrices having non-polar, more hydrophobic and relatively low free energy surfaces. Filler surface treatment can be applied for appropriate adhesion. Stearic acid [$CH_3(CH_2)_{16}COOH$] treatment has been known to improve processability, wettability and surface quality of $CaCO_3$.

1.3.2. Kaolin

Kaolin is a member of clay family. With the addition of kaolin, some properties of thermoplastic composites such as electrical properties, surface quality, chemical resistance and hardness can be improved. Kaolin also reduces the possibility of water absorption and crack growth [16].

1.3.3. Feldspar

Feldspar is a natural mineral which used in Polyvinyl chloride (PVC) and thermosets. It has some advantages such as translucency, wettability, higher flexural strength, modulus, chemical and abrasion resistance.

1.3.4. Hydrated Alumina

Hydrated alumina is a flame retardant and smoke suppressant filler. In order to achieve flame retardancy, large amounts of this material are needed [17].

1.3.5. Silica

Silica is the most abundant mineral on the earth's crust and it is used as a reinforcing filler in rubbers. Some advantages are high resistance to heat, low thermal coefficient, good electrical properties and transparency [17].

1.3.6. Talc

Talc is one of the most commonly used reinforcing filler for thermoplastics. It improves electrical performance, chemical, heat and moisture resistance.

1.3.7. Mica

Mica is commonly used as a reinforcing additive in polymeric or ceramic matrix. The addition of mica improves stiffness, warp resistance and dimensional stability of thermoplastic matrix.

1.3.8. Other Mineral Fillers

Other mineral fillers used for reinforcing thermoplastic matrix are summarized as follows [16]:

- Barium sulfate: Used for sound-damping panels due to its high density.
- Calcium sulfate: A reinforcing mineral filler used for polyolefins.
- Calcium silicate (wollastonite): Improves chemical and moisture resistance of thermoplastics.
- Titanium dioxide: Used as universal white pigment in paints.

CHAPTER 2

LITERATURE REVIEW

The effect of $CaCO_3$ particles on the mechanical properties of polymers has received the great attention of scientists in recent years. There have been many studies using nano sized calcium carbonate ($CaCO_3$) to enhance the properties of polymers. The following review summarizes some of these studies (Table 2.1).

2.1. Effect of $CaCO_3$ Particles on the Mechanical Properties of Polypropylene

Polypropylene is the one of the most important thermoplastic polymer which is widely used in technical applications due to its low cost, relatively high mechanical properties, recyclability. However, owing to its low modulus, poor impact resistance the usefullness of PP is still limited. For this reason increasing the impact toughness and modulus of PP has received considerable interest by the scientists.

$CaCO_3$ nanoparticles are very effective toughening agent for PP [18,19]. Impact strength of PP could be increased by adding mineral filler. Chan *et al.* [18] reported that impact strength of PP increased from 55 J/m to 133 J/m by adding 9.2 vol.% surfactant treated with an average diameter of 44 nm $CaCO_3$ [18].

Toughening of polypropylene with $CaCO_3$ particles, with the influence of particle size (0.07-1.9 μm) and particle content of 0-32 vol.% was studied by Zuiderduin et al. [19]. They reported that rigid particles leads to a system with higher stiffness and higher impact resistance.

The addition of nano-$CaCO_3$ particles with stearic acid surface treatment on the $CaCO_3$ particles, improves the mechanical properties of PP [20-31]. With increasing $CaCO_3$ particle content Tensile strength decreases, while Young's modulus increases. Microstructural analysis according to the Scanning Electron Microscopy (SEM) observations of the fracture surfaces of the samples revealed an improvement in $CaCO_3$ dispersion as a result of surface treatment [21]

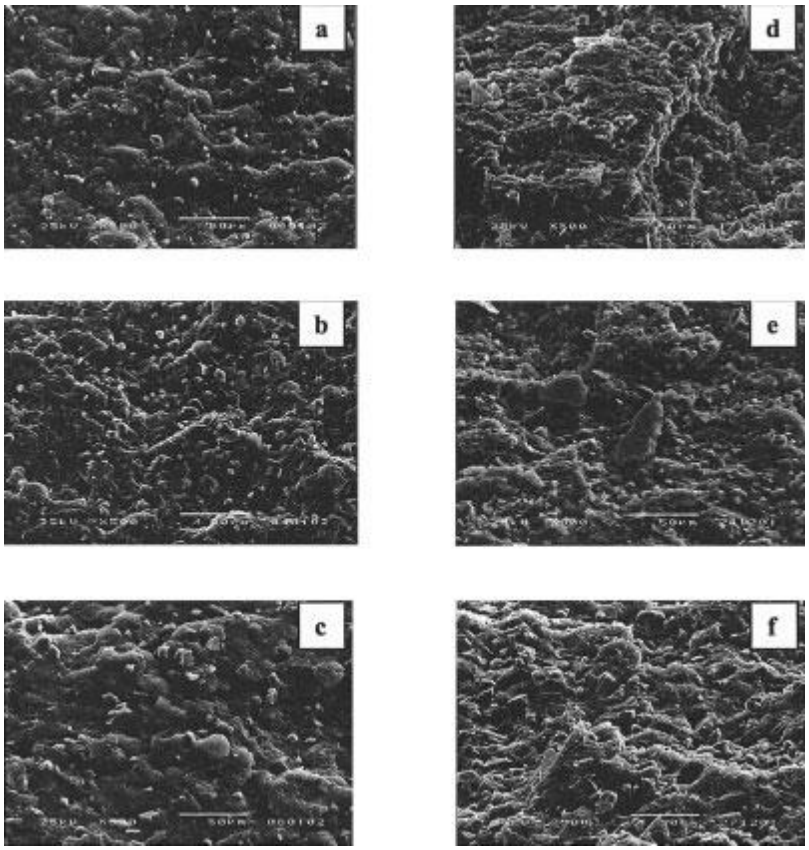

Figure 2.1. SEM micrographs of fractured surfaces of selected impact test specimens for s-PP filled with (a) 1.9, (b) 2.8, and (c) 10.5 μm , uncoated $CaCO_3$ particles at 20 wt % and (d) 1.9, (e) 2.8, and (f) 10.5 μm uncoated $CaCO_3$ samples at 40 wt % [21]

The crystallisation behaviour of $CaCO_3$ /PP nanocomposites were studied by a number of researchers [23,30]. Hanim et. al. [23] investigated the crystallization behaviour of nanocomposites by using Differential Scanning Calorimetry (DSC) technique. They showed that the addition of NPCC decreases crystallization temperature of PP.

Eiras et al. [24] investigated mechanical properties of $CaCO_3$/PP nanocomposites. The nanocomposites were prepared in a co-rotational twin screw extruder machine with calcium carbonate content of 3,5,7 and 10 wt. (%). They reported that there is an increase in PP elastic modulus and a little increase in yield stress. They suggested that the tensile properties depend on the surface contact area of nanoparticles and their dispersion. With the addition of relatively small content of $CaCO_3$ nanoparticles, they obtained a significant increase in elastic modulus and yield stress, although the addition of higher contents of nanoparticles did not lead to subsequently increase in these properties that remained constant.

Lam et al. [25] studied the effect of nanosized and surface-modified precipitated calcium carbonate on the properties of $CaCO_3$/polypropylene nanocomposites. It has been shown that a good dispersion of nano-PCC (precipitated calcium carbonate particles) in PP matrix was achieved. The thermal stability was increased. A strong interaction between nano-PCC (nano-sized and surface-modified PCC) and the PP matrix caused an increase in yield and tensile strength and the maxima were reached when loading 15–20 wt% of ns-PCC.

Ihueze and Mgbemena [26] examined the effect of calcium carbonate particles as a filler on the mechanical properties of polypropylene. They reported that the Young's modulus of the nanocomposite showed some improvement with the incorporation of the calcium carbonate nano-filler while the tensile strength deteriorated. The stearic acid coated fillers showed the highest improvement in the above tensile properties at low volume fractions while the deformation rate increases with the inclusion of the nanofiller.

Lin et al. [27**]** studied the toughening mechanism of polypropylene/calcium carbonate nanocomposites and the effect of the polymer molecular weight on the dispersion of nanoparticles. They reported that higher molecular weight polymer matrix does not affect the dispersion of nanoparticles and a monolayer coating is an effective way to improve the dispersion of nanoparticles. The notched Izod impact strength of the nanocomposites containing the high molecular weight PP and 20 wt% $CaCO_3$ nanoparticles with a monolayer coating of stearic acid was measured to be about 370 J/m, whereas the impact strength of the unfilled PP was 50 J/m.

Zhang et al. [28] studied the preparation and characterization of nano/micro-calcium carbonate particles/polypropylene composites. They prepared composites on a twin screw extruder with the nanoparticle content of 5% and 15 wt%. The sample which contains micro and nano sized particles shows the best mechanical property.

Buasri et. al. [29] investigated the effect of modified calcium carbonate ($CaCO_3$) nanoparticles on the thermal and mechanical properties of PP. Sodium stearate was used as a surface modifier. They modified the surface of nanoparticles to disperse them into the PP matrices without aggregation. $CaCO_3$ / PP nanocomposites with different filler content have been prepared by a co-rotating twin screw extruder and injection molding machine. The modified $CaCO_3$ improved the mechanical properties of PP effectively. The impact strength and hardness are increased by about 65% and 5%, respectively. The

morphology, investigated by Scanning Electron Microscopy (SEM), indicated that a uniform dispersion of filler in the polymer matrix

Zaman and Hun [30] studied the effect of surface-modified calcium carbonate nanoparticles on the mechanical properties and crystallization behavior of polypropylene. Pimelic acid (Pa) was used as a surface modifier for nano sized calcium carbonate (nCC). They prepared three compositions of PP/nCC composites in a co-rotational twin-screw extruder machine with nCC content of 5, 10, 15, and 20 wt%. According to the SEM results, the untreated nCC show a uniform size distribution for nCCPa, which dispersed well in PP. After surface modification by the Pa, the adhesion between the filler particles and PP matrix was enhanced and the aggregation could be avoided. The mechanical test results shows that the elastic modulus and impact strength of the composites increased at first and then decreased with the addition of fillers, and the tensile yield stress was reduced at the same time. They studied the crystallization properties of virgin PP and its composites with differential scanning calorimetry. The results shows that, in comparison with unfilled PP and PP/nCC, the addition of the Pa-treated nCC fillers into PP led to a higher crystallization temperature, and nucleation.

Zaman and Beg [31] investigated the mechanical, thermal, and rheological properties of nCC/ PP composites modified by methacrylic acid (MA). MA was used as a surface modifier for nCC. They prepared the nanocomposites by a twin screw extruder. MA effects on the morphology, mechanical properties, crystallization and melting behavior, and rheological properties of nCC/PP composites have been investigated. The SEM observation shows the surface treatment of nCC with MA improves the dispersion of the filler in the matrix. Differential scanning calorimetry results indicate that nCC has a heterogeneous nucletion effect on PP because of that the addition of nCC increased the crystallization temperature (T_c) of PP. In addition the mechanical tests indicate that nCC can simultaneously reinforce and toughen PP. Table 2.1 shows the recent studies carried on the effect of $CaCO_3$ particles on the mechanical properties of polypropylene.

Table 2.1. Summary of the literature survey on the effect of $CaCO_3$ particles on the mechanical properties of Polypropylene

Year	Reference	Effect of $CaCO_3$ particles on the mechanical properties of Polypropylene
2002	Chan et al. [18]	The modulus of the composites increased approximately 85% while the yield stress and strain were not much affected by the presence of $CaCO_3$ nanoparticles.
2003	Zuiderduin et al. [19]	The modulus of the composites increased, while the yield stress was lowered with filler content.
2003	Wang *et al.* [20]	Mechanical properties of PP were significantly increased by the incorporation of nano-$CaCO_3$ pretreated with stearic acid.
2004	Supaphol et al. [21]	Tensile strength decreased, while Young's modulus increased, with increasing $CaCO_3$ content. Surface treatment on $CaCO_3$ particles reduced tensile strength and Young's modulus, but improved impact resistance
2006	Yang et. al. [22]	Flexural strength and modulus of PP nanocomposites increased with increasing particle content
2008	Hanim et al. [23]	The impact strength and modulus of PP showed some improvement with the incorporation of the nanofiller while the tensile strength deteriorated
2009	Eiras et al. [24]	PP elastic modulus increased and a little increase in yield stress.
2009	Lam et al. [25]	Yield and tensile strength increased
2010	Ihueze and Mgbemena [26]	The stearic acid coated fillers showed the highest improvement in the above tensile properties at low volume fractions not exceeding 0.10 while the deformation rate increases with the inclusion of the nanofiller.
2010	Lin et al. [27]	The notched Izod impact strength of the nanocomposites containing the high molecular weight PP and 20 wt% $CaCO_3$ nanoparticles with a monolayer coating of stearic acid was measured to be about 370 J/m, whereas the impact strength of the unfilled PP was 50 J/m.
2011	Jun Zhang et al. [28]	In the process of impact the nanoparticles could create microcavitation and this is an important process of absorbing energy in impact while PP was filled with nano $CaCO_3$
2012	Buasri et. al. [29]	The impact strength is increased by about 65%.
2012	Zaman and Hun [30]	Elastic modulus and impact strength of the composites increased at first and then decreased with the addition of fillers, and the tensile yield stress was reduced at the same time.
2014	Zaman and Beg [31]	$CaCO_3$ can simultaneously toughen PP

2.2. Effect of $CaCO_3$ Particles on the Mechanical Properties of Polyethylene

Kwon et al. [32] investigated the mechanical properties and complex melt viscosity of unfilled and the calcite filled high density polyethylene (HDPE), low density polyethylene (LDPE), and linear low density polyethylene (LLDPE) composites. They prepared the composite samples by using a twin-screw extruder. They also added anti-oxidant and UV-stabilizer to prevent the composites from oxidation and UV absorption. The tensile stress and the complex melt viscosity of the calcite filled polyethylene composites were higher than that of unfilled PE, implying that the reinforcing effect of calcium carbonate.

Kundu et al. [33] studied the investigation of the comparative tensile and impact properties and fracture morphologies between calcite and calcite/zeolite (hybrid) filled linear low-density polyethylene (LLDPE) and polypropylene (PP) composites. The incorporation of fillers into LLDPE, whether calcite or calcite/zeolite hybrid fillers, does not alter the T_m of LLDPE, but slightly reduces the T_m of PP. The impact strength, Young's modulus, and yield stress of the calcite and the hybrid filled LLDPE increased, indicating a reinforcing effect of the fillers. In addition, the elongation at break (EB) and ultimate tensile strength of the filler LLDPE decrease. However, the hybrid LLDPE composite exhibits slightly higher Young's modulus and ultimate tensile strength than the calcite one, while the same values of impact strength and yield stress were observed. In the PP system, the Young's modulus is enhanced, whereas the rest of the mechanical properties were reduced.

Misra et al. [34] studied the surface deformation and fracture process during during tensile loading of 5–20 wt. % calcium carbonate-reinforced polyethylene composites and they compared the behavior with unreinforced neat polyethylene as a function of strain rate of tensile test. Calcium carbonate reinforced polyethylene composites exhibit increased tensile modulus in comparison to neat polyethylene. The reinforcement of neat polyethylene with 5–20% calcium carbonate increased the tensile modulus. However, a distinct effect on yield strength was not observed. The addition of calcium carbonate to neat polyethylene enhanced the crystallization to a small extent, but the increase in percent bulk crystallinity was significant.

Deshmane et al. [35] investigated the mechanical response of calcium carbonate-reinforced high density polyethylene nanocomposite. They compared the mechanical

behavior of composites with the unreinforced polyethylene processed under similar conditions. The incorporation of nano-scale calcium carbonate into high density polyethylene demonstrated reinforcement effects that contribute to the increase in bulk crystallinity and modulus of the material, while the nucleating effect decreases the spherulite size and enhances toughness. The achievement of high impact strength is accompanied by increase in modulus and no loss in yield strength. The reinforcement of neat high density polyethylene (HDPE) with nano-calcium carbonate alters the deformation micromechanism from crazing–tearing in HDPE to fibrillated fracture in polymer nanocomposite.Schrauwen et al.[36] investigated the impact toughness of high density polyethylene with calcium carbonate particles for different processing conditions. The influence of crystal orientation was investigated. They found that hard filler particles are effective to improve impact toughness of HDPE. A large increase in toughness can be obtained by creation of a crystal oriented structure. Elleithy et al.[37] examined the morphological, thermal, and viscoelastic properties of high density micro calcium carbonate/polyethylene composites. They prepared the composites on a twin screw extruder and they molded samples by an injection molding. The morphological analysis revealed that the $CaCO_3$ agglomerated. The Thermogravimetric analysis (TGA) of the composite samples showed that the thermal stability of the composites increased as indicated by the increase of the onset degradation temperature. The addition of $CaCO_3$ microparticles did not affect the shear sensitivity of the composite, but it increased the viscosity as compared to the neat resin. Table 2.2 shows the recent studies carried on the effect of $CaCO_3$ particles on the mechanical properties of polyethylene.

Table 2.2. Literature survey on the effect of $CaCO_3$ particles on the mechanical properties of Polyethylene

Year	**Reference**	**Effect of $CaCO_3$ particles on the mechanical properties of Polyethylene**
2002	Kwon et al [32]	The tensile stress increased.
2002	Kundu et al. [33]	The impact strength, Young‟s modulus, and yield stress of the calcite and the hybrid filled LLDPE increased.
2004	Misra et al. [34]	Increased tensile modulus however, a clear discernible effect on yield strength was not apparent.
2007	Deshmane et al. [35]	The achievement of high impact strength is accompanied by increase in modulus and no loss in yield strength.
2008	Schrauwen et al [36]	Improved impact toughness of HDPE and a large increase in toughness.
2010	Elleithy et al [37]	The presence of $CaCO_3$ increased the shear modulus at low frequency of the composites at 80°C over that of the neat resin.

Although the studies on the effect of $CaCO_3$ particles on the mechanical properties of polymer composites have been covered extensively in the literature, there is limited information on the mechanical properties of nano-$CaCO_3$ filled composites.

CHAPTER 3

MANUFACTURING OF FILLED THERMOPLASTIC COMPOSITES

Polymer processing is used for converting solid and/or liquid polymers to finished products. It consists of three steps; (*i*) pre-shaping (melt mixing, softening, pumping etc.), (*ii*) shaping (molding, casting, etc.), (*iii*) post-shaping (decorating, fastening, etc.) [38].

In this study, a twin screw extrusion machine was used for polymer melting and homogeneous mixing of polymers with inorganic fillers. To obtain the test specimens, injection molding process was used.

3.1. Extrusion

Extrusion process is performed by forcing a material through an orifice to create an extrudate. Different materials can be formed into profiles by using extrusion process including metals, polymers and ceramics.

Polymers are extruded in solid or molten state. A polymer (in a powder or granular form) is put in a hopper. A screw thread turns forcing the plastic material through a heater, melting it within the extruder in a process called plasticating extrusion. When all the material melts, the screw thread then acts as a ram and forces the material through a die and then extrudate cooled in a water bath (Figure 3.1) [16].

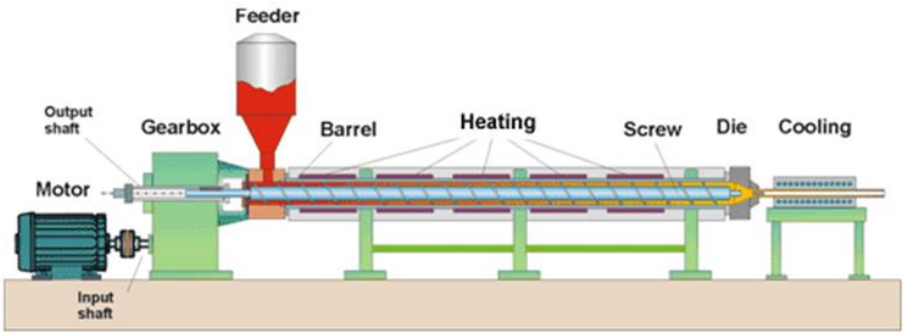

Figure 3.1. Extrusion process [39]

3.1.1. Extrusion Terminology

Some important terms about extrusion process are briefly explained in the followings:

- *Barrel* : A cylindrical housing in which the screw rotates; including liner, if used.
- *Screw* : A helically flighted shaft which when rotated mechanically works and advances the material being processed.
- *Screw speed* : Number of revolutions of screw per minute. The term is widely known as ‘rpm’.
- *Extruder length to diameter ratio, L/D* : The distance from the forward edge of the feeder opening to the forward end of the barrel.
- *Feed section of screw* : The portion of a screw, which picks up the material at the feed opening plus an additional portion downstream.
- *Compression section of screw* : The portion of a screw between the feed section and metering section in which the flight depth decreases in the direction of discharge.
- *Metering section of screw* : The metering zone is the final part of the screw and acts rather as a metering pump from which the molten plastics material is delivered to the die system at constant volume and pressure.

3.1.2. Extruder Classification

Extruders are divided into two basic categories: *continuous* and *discontinuous*. Continuous extruders contain a rotating part such as a disc, drum or a screw to develop a steady continuous flow of material. Discontinuous extruders generally utilize a reciprocating ram to push material through the die [40].

3.1.2.1. The Single-screw Extruder

The single-screw extruder consists of a single screw rotating in a heated metal barrel. During process, a solid material enters the barrel from a hopper and transferred by the screw into a heated region of the barrel. As the solid feed continues along the barrel, it is softened and mixed to form a homogenous melt. The solid is then pumped through the die. Figure 3.2 shows the schematic representation of a single-screw extruder.

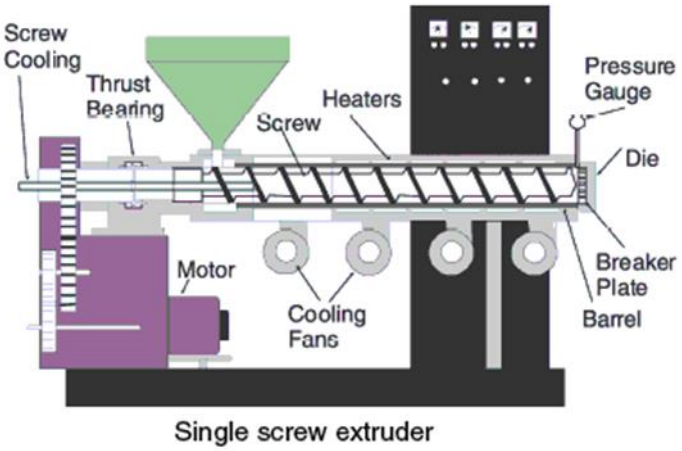

Figure 3.2. Schematic representation of a single-screw extruder [41]

3.1.2.2. Twin-screw Extruders

A twin-screw extruder contains two screws within a single barrel. There are two types of twin screw extruders; co-rotating and counter-rotating. For each class of extruder, the flights may or may not be intermeshing (Figure 3.3) .

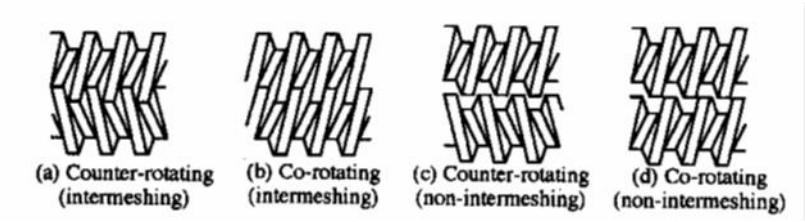

Figure 3.3. Twin-screw extruder profiles [40]

The main difference between a single and twin-screw is the type of their flow pattern. Twin-screw extruders have many processing advantages over single screw extruders. For instance, the larger heat transfer area offers better temperature control and superior feeding characteristics, shorter and more controlled residence times for the melt in the barrel. Therefore, twin-screw extruders improve processing capability of thermally unstable polymers. A relatively common twin-extruder is the melt gear-pump, which is essentially a specialized type of closely intermeshing and counter-rotating twin-screw extruder [40].

3.1.2.2.1. Intermeshing Counter-rotating Extruders

High pressures are generated between the screws due to the positive pumping characteristics of closely intermeshing counter-rotating extruders. Therefore, screw speeds are restricted to prevent possible screw deflection. However, the extruder can be operated at higher speed when the degree of conjugation is reduced. Therefore, the maximum allowable screw speed of an intermeshing counter-rotating extruder is between 100-200 rpm which indicates relatively poor positive pumping ability [16].

3.1.2.2.2. Intermeshing Co-rotating Extruders

Intermeshing co-rotating extruders are designed for special purposes requires efficient mixing characteristics such as compounding, blending, devolatilization and chemical modification of thermoplastics. The maximum allowable screw speed of an intermeshing co-rotating extruder is between 300-600 rpm.

3.1.2.2.3. Non-Intermeshing Extruders

In non-intermeshing extruders, the screw lengths of the two shafts can be equal or one screw can be longer than the other to provide better melt pumping capability. Non-intermeshing extruders are used for devolatilization, chemical reactions [42].

3.2. Injection Molding

Nowadays, injection molding is being widely used for manufacturing parts with variable dimensions. It is one of the most important manufacturing method for converting thermoplastic and thermosetting materials into all types of products. The process is based on the ability of the thermoplastics to be softened by heat and to be hardened when cooled.

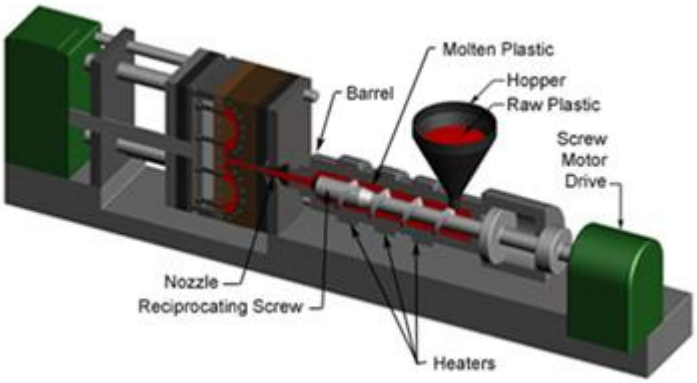

Figure 3.4. A typical injection moulding machine [43]

Figure 3.4 shows a typical injection moulding machine. The clamping unit keeps mold parts together during injection of molten plastic and cooling time. Injection unit is composed of hopper; heat controlled barrels-cylinder, screw and motor. Mold is the place where the molten polymeric material is shaped. During the injection process, thermoplastic pellets are fed from a hopper on top of the injection unit. The pellets are fed into the cylinder by the reciprocating movement of the screw and heated until they melt. The process begins with the accumulation of melted plastic in front of the screw. The speed controlled screw forces molten plastic forward into the mold cavity and then holds the force to minimize the shrinkage of molded part. After finishing injection and holding the pressure, the mold is kept closed until the cooling is completed. When the cooling is completed, mold is opened and the ejectors force the molded-shaped parts out. In this study, a single screw injection molding machine is used for manufacturing test specimens.

CHAPTER 4

MECHANICAL BEHAVIOR OF FILLED THERMOPLASTIC COMPOSITES

Mechanical testing plays an important role in evaluating fundamental properties of engineering materials. If an engineering structure is subjected to loading, it is vital to know how strong and rigid the material is. Therefore, engineers have developed a number of experimental techniques [44].

4.1. Tensile Test

In this test, a specimen is mounted into the jaws of the testing machine and uniaxial tension load is applied. The cross section of the specimen is usually round (for metals), or rectangular (for polymers). Figure 4.1 shows tensile test specimens having different cross-sectional area. The central cross-section of the specimen is smaller than the final cross-section ensure that the specimen fails in the gauge length.

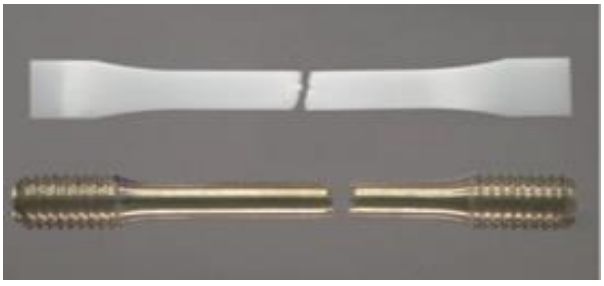

Figure 4.1. Tensile test specimens having (a) rectangular and (b) round cross section [45]

During the test, the load- elongation curve is plotted by means of a load all and extensometer. The tensile behavior of the material is obtained. The engineering stress-strain curve of the material is constructed by making the required calculations on this load-elongation curve.

The major parameters that describe the stress-strain curve are: the tensile strength (UTS), yield strength or yield point (σ_y), elastic modulus (E), percent elongation (ΔL%) and the reduction in area (RA%). The data obtained from the tensile tests describes many mechanical features of the material. Toughness, resilience and poisson's ratio (v) can be also found. The calculation of some of these parameters is explained as follows [46]:

Engineering stress is obtained by using Eq. (4.1). The load (P) is divided by the original area of the cross section (A_0) of the specimen.

$$\sigma = \frac{P}{A_0} \tag{4.1}$$

Engineering strain can be calculated as follows:

$$\varepsilon = \frac{\Delta l}{l_0} \tag{4.2}$$

where l_0 and Δl are the initial gage length and elongation, respectively.

In a stress-strain curve, there are two main deformation regions which are elastic and plastic regions. In the elastic region, stress and strain are related to each other linearly. The elastic modulus (E) which is specific for each type of material can be calculated by using Eq. (4.3).

$$E = \frac{\sigma}{\varepsilon} \tag{4.3}$$

Ultimate tensile strength (UTS) is the maximum stress that the material can withstand. It can be calculated by using Eq. (4.4) given below:

$$\sigma_{UTS} = \frac{P_{\max}}{A_0} \tag{4.4}$$

Where P_{max} is maximum applied load.

Yield strength (σ_y) is the stress level at which plastic deformation starts. The beginning of first plastic deformation is called yielding. It is an important parameter in design.

4.1.1. Tensile Behavior of a Polymeric Material

Figure 4.2. below shows a typical stress-strain curve of a polymeric material.

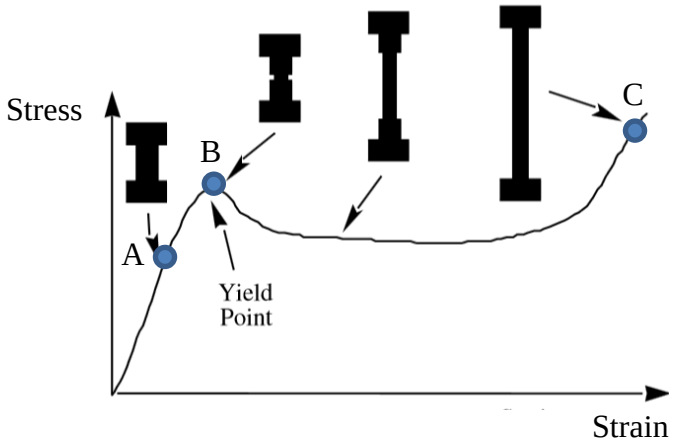

Figure 4.2. A typical stress-strain curve of a polymeric material [47]

At low stresses and strains, the polymeric material behaves like a linear elastic solid. The point A where the behaviour starts to be non-linear is called the proportional limit. The local maximum in the stress-strain curve is called the yield point and indicates the onset of plastic (i.e. permanent) deformation. The corresponding stress and elongation are called yield strength and elongation at yield (point B) [47].

Beyond the yield point, a "neck" is formed; this region is called the plastic region. Due to straightening of polymer chain, an abrupt increase in stress is observed and further elongation causes the ultimate rupture of the material. The corresponding stress and strain are called the ultimate strength and the elongation at break, respectively (point C).

The stress-strain behaviour of a polymeric material depends on some parameters such as molecular characteristics, microstructure, strain-rate and temperature. Figure 4.3 shows the comparison of LDPE and HDPE stress-strain curves. HDPE has a higher

degree of crystallinity than the low density grade, therefore, yield strength and stiffness of HDPE are higher than those of LDPE.

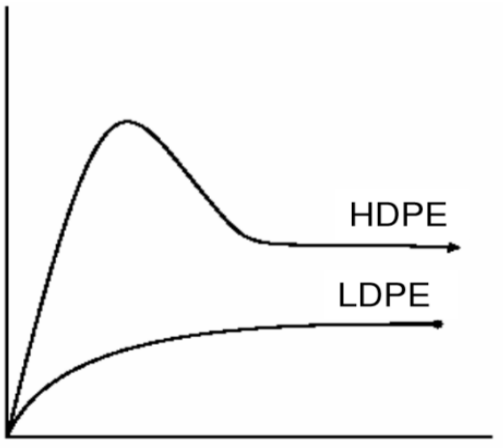

Figure 4.3. Comparison of LDPE and HDPE stress-strain curves [47]

4.1.2. Deformation Mechanisms of Filled Polymers

An increase in filler content causes a transition of failure modes from ductile to brittle (Figure 4.4). Fracture strain of a filled polymer is lower than that of the unfilled polymer. In addition, filler may prevent necking and initiate yielding in craze-like zones. In filled polymers at least six modes of deformation behavior can be observed: 1) brittle, 2) quasibrittle fracture during neck formation, 3) fracture during neck propagation, 4) stable neck propagation, 5) uniform yielding, and 6) yielding in crazes [13].

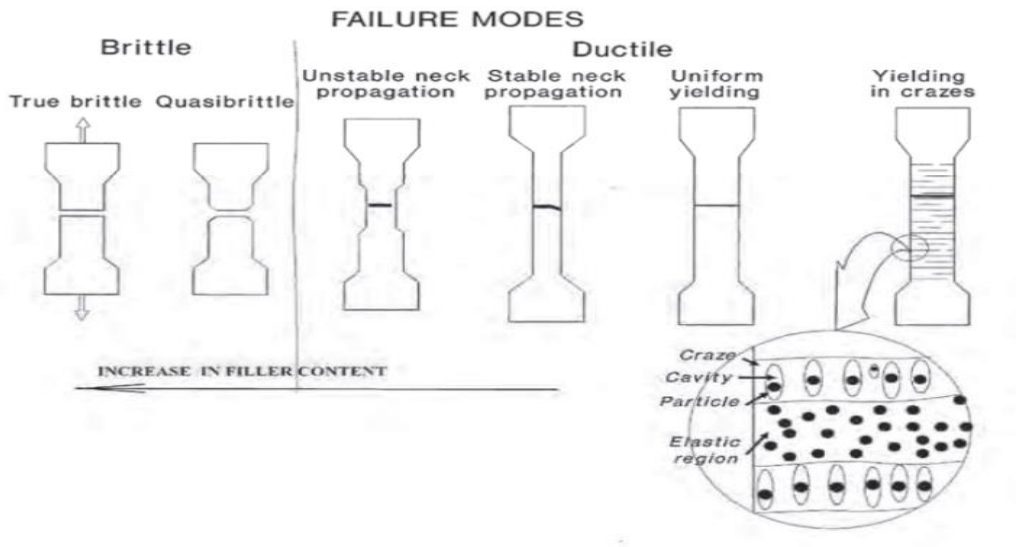

Figure 4.4. Fracture modes of filled polymers [13]

4.2. Flexural Test

Flexural testing is a mechanical test in which the specimen having standardized geometry is supported at it ends. The load is applied in the center of the specimen under standardized conditions (Figure 4.5). The force is measured and recorded during the deformation (bending).

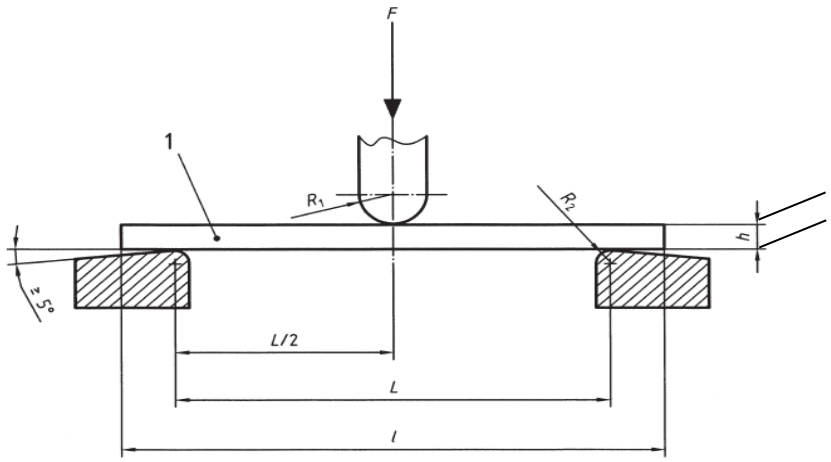

Key

1	Test specimen	h	Thickness of specimen
F	Applied force	l	Length of specimen
R_1	Radius of loading edge	L	Length of span between supports
R_2	Radius of supports		

Figure 4.5. Position of test specimen at beginnig of test [48]

The flexural strength(σ_f) can be calculated as follows [48]:

$$\sigma = \frac{3FL}{2bh^2} \tag{4.5}$$

where F is the applied force. L, b and h are the span, width and thickness of the specimen, respectively. To determine the flexural modulus (E_f), the deflections s_1 and s_2 corresponding to flexural strain ε_1=0.0005 and ε_2=0.0025 are calculated by using Eq. (4.6) [48];

$$s_i = \frac{\varepsilon_{fi} L^2}{6h} \tag{4.6}$$

The flexural moduls (E_f) is calculated as follows [48]:

$$E_f = \frac{\sigma_{f2} - \sigma_{f1}}{\varepsilon_{f2} - \varepsilon_{f1}} \tag{4.7}$$

4.3. Charpy Impact Test

The Charpy impact test, also called Charpy V-notch test, is a standardized high strain-rate test that one can obtain the amount of energy absorbed by a material during fracture. This absorbed energy is a measure of a given material's toughness. It is widely used in industry, since it is easy to prepare and conduct and results can be obtained quickly and cheaply.

In this test, a hammer like weight strikes a specimen and the energy to break is determined from the loss in the kinetic energy of the hammer. The specimen can be a notched or unnotched bar. Figure 4.6 shows a schematic representation of Charpy impact test.

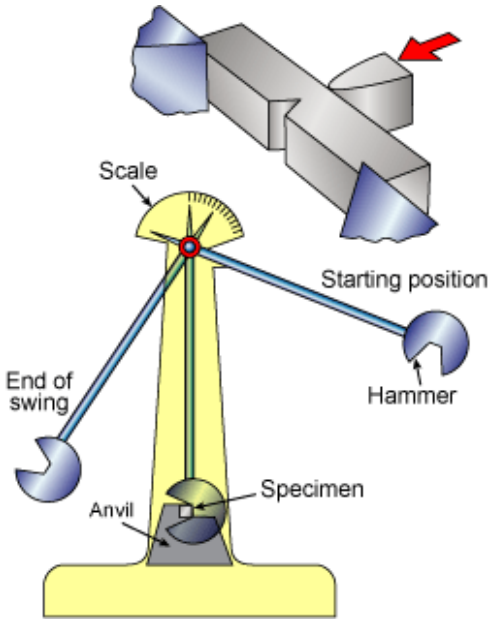

Figure 4.6. Schematic representation of Charpy impact test with a notched bar [49]

The Charpy impact strength can be calculated by using Eq. (4.8) [50];

$$a_{cN} = \frac{E_c}{hb_n}.10^3 \qquad (4.8)$$

Where E_c is the corrected energy in Joules, h and b_n are the thickness and remaining width respectively.

CHAPTER 5

EXPERIMENTAL

5.1. Materials

5.1.1. Polyethylene

Polyethylene pellets were used as a base polymer of the matrix to produce $CaCO_3$ / PE nanocomposites. The polyethylene pellets were kindly supplied by Petkim Petrochemistry, Turkey under the trade name PETİLEN YY S 0464. The physical properties of polyethylene is given in Table 5.1.

Table 5.1. Physical Properties of Polyethylene

Property	Test Method	Unit	Value
Melt Flow Rate (190°C, 160g)	ASTM D1238	g/10 min	0.36
Density at 23°C	ASTM D1505	g/cm^3	0.961
Tensile Strength at Yield	ASTM D638	MPa	28
Tensile Strength at Break	ASTM D638	MPa	31
Elongation at break	ASTM D638	%	1115
Flexural Modulus, 23°C	TS EN ISO 178	MPa	1000
Izod Impact Strength	ASTM D256	MPa	590
Melting Point (DSC)	ASTM D3417	**°C**	134

5.1.2. Polypropylene

Polypropylene pellets were used as a based polymer of the matrix to produce $CaCO_3$ /PP composites. The trade name of polypropylene used in this work is PETOPLEN MH-418. The polypropylene pellets were supplied by Petkim Petrochemistry, Turkey. Table 5.2. shows the physical properties of polypropylene.

Table 5.2. Physical Properties of Polypropylene

Property	Test Method	Unit	Value
Melt Flow Rate (190°C, 160g)	ASTM D1238	g/10 min	4.5
Density at 23°C	ASTM D1505	g/cm^3	0.905
Tensile Strength at Yield	ASTM D638	MPa	34
Tensile Strength at Break	ASTM D638	MPa	42
Flexural Modulus at 23°C	TS EN ISO 178	MPa	1420
Izod Impact Strength	ASTM D256	MPa	21.6
Melting Point (DSC)	ASTM D3417	**°C**	163

5.1.3. Calcium Carbonate ($CaCO_3$)

5.1.3.1. $CaCO_3$ with and without surface treatment

In this study, $CaCO_3$ particles with stearic acid surface treatment and without surface treatment were used as a filler. They were supplied from ADAÇAL Inc, Afyon, Turkey under the trade name "*N1 and N1-C"*. The chemical composition and physical properties of the fillers are illustrated in Table 5.3 and 5.4 respectively.

Table 5.3. Chemical Composition of $CaCO_3$ Particles

Composition (wt %) / **Materials (%)**	**$CaCO_3$ Particles**	
	Without surface treatment	**With SA surface treatment**
$CaCO_3$	99.35	99.35
MgO	0.17	0.17
Fe_2O_3	0.08	0.08
SiO_2	0.22	0.22
SO_3	0.12	0.12
Na_2O	0.06	0.06

Table 5.4. Physical Properties of $CaCO_3$ Particles

Property	Method	Value	
		$CaCO_3$ (without surface treatrment)	**$CaCO_3$ (with stearic acid surface treatment)**
Average Particle Size	SEM	50 nm	50 nm
Density	ASTM D-5550-06	2.94 g/cm^3	2.84 g/cm^3
pH	ISO787-9	9.1	9.1
Surface area	TS ISO 9277	21.48 m^2/g	17.92 m^2/g

5.2. Characterization of $CaCO_3$ Particles

5.2.1. Microstructural Features

5.2.1.1. X-Ray Diffraction (XRD)

The crystallinity of $CaCO_3$ nanoparticles was characterized by X-ray Diffraction (XRD) analysis using a Phillips™ Xpert diffractometer with Cu Kα as a radiation source. Powdered sample were scanned in the interval of a $2\theta = 5°\text{-}80°$ at 45 kV and 40 mA, at scanning speed of 2^o/min.

5.2.1.2. Scanning Electron Microscopy (SEM)

$CaCO_3$ nanoparticles were investigated with Scanning Electron Microscopy (SEM), (Phillips™ XL-30S FEG). All the sample surfaces were gold-coated by a sputtering apparatus before the SEM examination to eliminate charging.

5.3. Characterization of Polymers

5.3.1. Thermal Properties of Polyethylene and Polypropylene

5.3.1.1. Differential Scanning Calorimetry (DSC)

Thermal properties of Polypropylene and Polyethylene, such as crystallization temperature and melting temperature were measured using a TA instrument Q10 with a heating rate of 10°C/min. Initially, the polymers were heated from -10^{o}C to 300°C for measurement of melting and held 5 min to erase the thermal history, then cooled to -10^{o}C for measurement of crystallization. Heat flow versus temperature graph was obtained. The change from the base line of this endothermic curves was detected as melting reaction and the exothermic curve obtained during cooling is detected as crystallization. The melting temperature (T_m) and crystallization temperature (T_c) were obtained. The start and end point of crystallization peak (T_{cs} and T_{cf}) and the peak value (T_c) are noted as crystalline temperature. The area below the crystallization peak enveloped by base line is recorded as heat of fusion.

5.3.1.2. Thermogravimetric Analysis (TGA)

In order to analyze the weight loss of Polypropylene and Polyethylene as a function of temperatures, thermogravimetric analysis (TGA) was performed by using a Perkin Elmer Diamond thermo gravimetric analyzer. The experiments were carried out from 25^{o}C to 600 ^{o}C at a heating rate of 10 ºC/min in a 50 ml/min nitrogen flow.

5.4. Characterization of Composites

5.4.1. Morphology Investigation

5.4.1.1. Scanning Electron Microscopy (SEM)

Examination of the microstructure of the polymeric nanocomposites and dispersion of the nanoparticles in the polymer matrix was identified by means of a scanning electron microscope (SEM), Phillips™ XL-30S FEG. In the purpose of preventing electron charge accumulation on samples, the gold sputtering technique was applied to the samples before the SEM analyses to have a conductive a thin gold layers on the surfaces.

5.4.2. Thermal Properties

5.4.2.1. Differential Scanning Calorimetry (DSC)

Crystallization temperature (T_c) and melting temperature (T_m) of the $CaCO_3$ /PP and $CaCO_3$ / PE nanocomposites were measured using a TA instrument Q10 with a heating rate of 10°C/min. Previously, the samples were placed in an aluminium crucible and heated from -10^o to 300° at a heating rate of 10° C/min., then held at that end temperature for 5 minutes. The reason for this first thermal cycle is to remove the crystalline elements of the specimen that could modify the crystallication kinetics of the specimen. The specimens were than cooled at a cooling rate of 10°C/min to -10°C below the final crystallization temperature of the specimens. The melting temperature (T_m) and the crystallization temperature (T_c) of nanocomposites were taken at the peaks of the melting and crystallization process, respectively.

5.4.2.2. Thermogravimetric Analysis (TGA)

In order to analyze the weight loss of PP/$CaCO_3$ and PE/$CaCO_3$ nanocomposites as a function of temperatures, thermogravimetric analysis (TGA) was performed by

using Perkin Elmer Diamond thermo gravimetric analyzer at the range of temperature of 25 ^{o}C to 600 ^{o}C at a heating rate of 10 ºC/min in a 50 ml/min nitrogen flow.

5.4.3. Measurement of Mechanical Properties

5.4.3.1. Tensile Test

Tensile tests were conducted on dumbbell shaped specimens with a Shimadzu AG-I 50 kN tensile tester (Figure 5.1). At least 5 specimens were tested for each composite configurations. Video extensometer was used to measure the strain during the tensile test. The test speed was kept at 30 mm/min. Prior to the measurement, the thickness and width of the specimen were measured with a micrometer and the cross-sectional area was calculated.

During the test, the force was recorded versus nominal strain. The Young's modulus of the samples was determined at 0.5 % strain. The tests were conducted until 150% of deformation. An average of five measurements for each sample is reported.

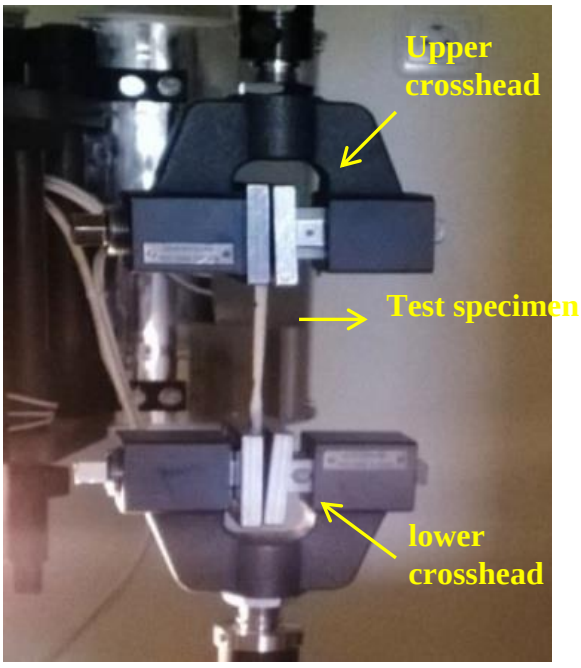

Figure 5.1. Tensile test specimen during test

5.4.3.2. Flexural Tests

The flexural behavior of the prepared specimens was investigated in accordance with EN ISO-178. For flexural tests, a three-point loading system was used, and the support span length was adjusted to 64 mm, the crosshead speed was 2 mm/min. At least five specimens from the composites were tested using the universal test machine. Force vs. deflection at the center of the beam was recorded. A test specimen under load is given in Figure 5.2.

Figure 5.2. Specimen under three point bending, (a) before loading, (b) during loading

5.4.3.3. Charpy-Impact Test

Charpy impact test machine (Ceast Resil Impactor) was used to determine toughness of $CaCO_3$/PP and $CaCO_3$/PE composite materials. This test was performed in accordance with ISO 179 standard. 80 mm long, approximately 4 mm thick and 10 mm wide specimens were tested. A Notch with a depth of 2 mm was opened on the specimen by using a notch opening apparatus. The test machine and notch opening apparatus are shown in Figure 5.3.

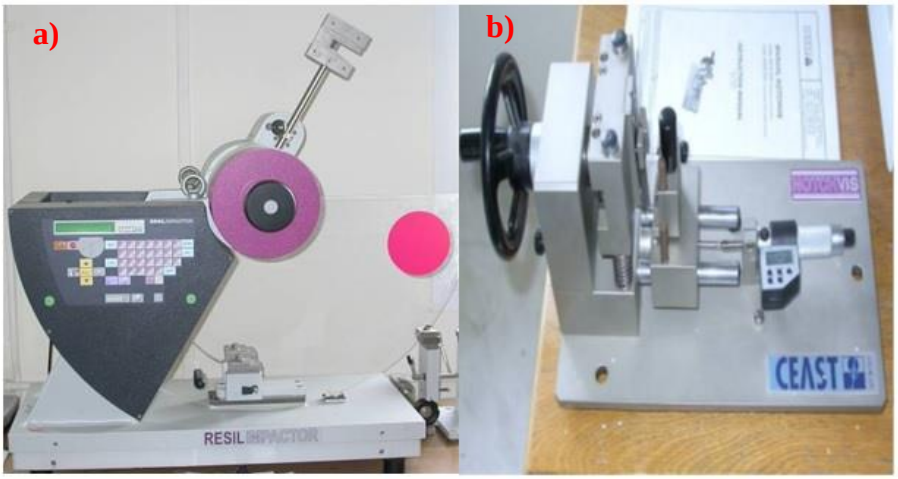

Figure 5.3. (a) Charpy impact machine and (b) notch opening apparatus

5.5. Preparation of Test Specimens

Calcite ($CaCO_3$) is a humidity sensitive material. Therefore, calcite was dried for 3 hours at 80 ^oC in an drying owen. This drying step was done within an air-circulating oven shown in Figure 5.4**.** After the drying procedure, calcite was cooled down to the room temperature.

Figure 5.4. Air-circulating oven used in drying process

Compounding recipes was done by using, 'THERMOFISHER (Eurolab 16mm)' co-rotating twin-screw extruder with the screw diameter 16 mm and L/D ratio 40 was used (Figure 5.5). The specifications of THERMOFISHER (Eurolab 16 mm) co-rotating twin-screw extruder are illustrated in Table 5.5. Barrel temperatures and screw speeds are shown in Table 5.6.

Figure 5.5. Thermofisher (Eurolab 16 mm) twin-screw extruder

Table 5.5. Specifications of twin screw corotational extruder

Thermofisher (Eurolab 16 mm)	**Unit**	**Value**
Screw Diameter	mm	16
Maximum Screw Speed	rpm	500
Barrel length	mm	640
L/D		40
Drive Power	kW	1.25 (Constant Torque)
Max Torque /shaft	Nm	12
Max Operating temperature	^{o}C	400
Max Operating Pressure	bar	100

Table 5.6. Barrel Temperatures (°C)

Material	**Screw Speed (rpm)**	**Barrel Temperatures (°C)**									
$CaCO_3$/PP	125	130	140	160	170	180	190	200	200	180	180
$CaCO_3$/PE	125	150	160	170	180	190	190	190	190	200	200

Polymer pellets were fed through the first feeder and then filler was fed from the second feeder. To investigate the effect of the filler on the thermoplastic materials, filler percentage varied between 0 and 30 % by weight (0, 5, 10, 15, 20, 25, 30 wt.%). To obtain effective mixture of intermeshing compounds extrusion step was repeated.

Designation of the $CaCO_3$ / PP and $CaCO_3$/ PE nanocomposites are given below in the Table 5.7 and 5.8, respectively. Composite materials (extrudate) were left the

extruder as spaghettis and they were cooled down to room temperature in a water bath and then cut into small pellets by a pelletizer shown in Fig 5.6.

Figure 5.6. Pelletizer

Table 5.7. Designation of the $CaCO_3$ /PP Composites Produced in Extrusion Process

Specimen code	**Coated $CaCO_3$ (wt.%)**	**Uncoated $CaCO_3$ (wt.%)**	**PP (wt.%)**
pp	0	0	100
5-uc-pp	0	5	95
10-uc-pp	0	10	90
15-uc-pp	0	15	85
20-uc-pp	0	20	80
25-uc-pp	0	25	75
30-uc-pp	0	30	70
5-c-pp	5	0	95
10-c-pp	10	0	90
15-c-pp	15	0	85
20-c-pp	20	0	80
25-c-pp	25	0	75
30-c-pp	30	0	70

Table 5.8. Designation of the $CaCO_3$/PE Composites Produced in Extrusion Process

Specimen code	**Coated $CaCO_3$ (wt.%)**	**Uncoated $CaCO_3$ (wt.%)**	**PE (wt.%)**
pe	0	0	100
5-uc-pe	0	5	95
10-uc-pe	0	10	90
15-uc-pe	0	15	85
20-uc-pe	0	20	80
25-uc-pe	0	25	75
30-uc-pe	0	30	70
5-c-pe	5	0	95
10-c-pe	10	0	90
15-c-pe	15	0	85
20-c-pe	20	0	80
25-c-pe	25	0	75
30-c-pe	30	0	70

The prepared extrusion blends were moulded into tensile, flexural and impact test specimens using an injection moulding machine (Figure 5.7).

Figure 5.7. Injection moulding machine

5.5.1. Tensile Test Specimen

Dog-bone shaped tensile test specimens were manufactured by the injection moulding machine. The mold is shown in Figure 5.8. The injection temperature of each barrel was set at 200^{o}C.

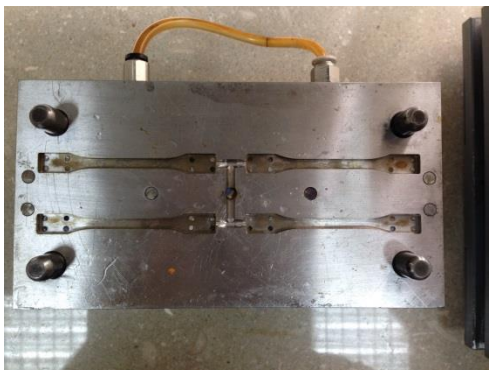

Figure 5.8. Tensile test specimens mold

5.5.2. Flexural and Impact Test Specimen

Flexural and impact test specimens with the dimensions of 80mm x 10mm x 4mm were manufactured by injection moulding machine. The injection temperature of each barrel was set at 200^{o}C. The mold used is shown in Figure 5.9.

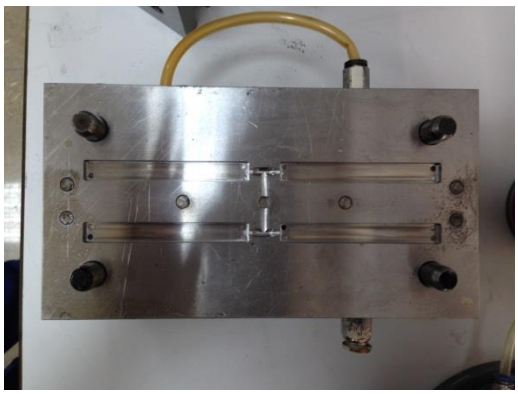

Figure 5.9. Flexural and impact test specimens mold

CHAPTER 6

RESULTS AND DISCUSSIONS

In this chapter, the thermal and microstructural features of the thermoplastic composites within the study are given. The characterization of filler materials ($CaCO_3$ with and without stearic acid surface treatment) and polymers (polyethlyene and polypropylene) used to prepare the thermoplastic composites are also reported. In addition, the microstructure, thermal and mechanical properties of the thermoplastic composites and preparation of samples reported.

6.1. The Investigation of $CaCO_3$ Particles Properties

6.1.1. Microstructural Features

6.1.1.1. X-Ray Diffraction (XRD)

XRD pattern of $CaCO_3$ particles without surface treatment is shown in Figure 6.1. XRD pattern of $CaCO_3$ particles with stearic acid surface treatment is shown in Figure 6.2. XRD patterns of both nanoparticles exhibited sharp peaks at $2\theta = 30°$. The peak for coated $CaCO_3$ has higher intensity values compared to those for the uncoated $CaCO_3$.

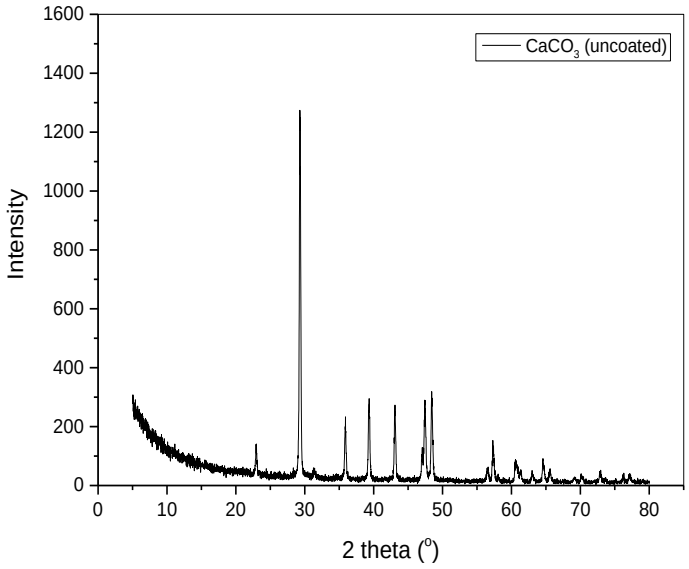

Figure 6.1. XRD pattern of $CaCO_3$ particles without surface treatment

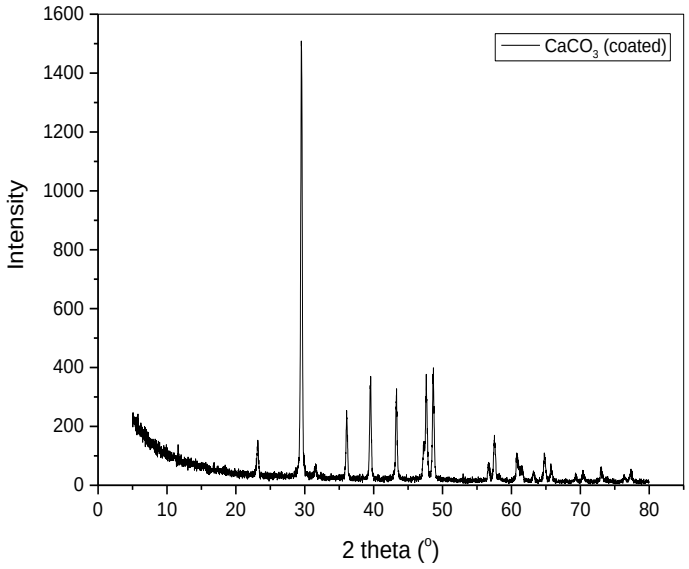

Figure 6.2. XRD pattern of $CaCO_3$ particles with stearic acid surface treatment

6.1.1.2. Scanning Electron Microscopy (SEM)

The SEM images of $CaCO_3$ particles without surface treatment is shown in Figure 6.3. Some aggregates can be seen in the figure. The SEM images of $CaCO_3$ particles with stearic acid surface treatment is shown in Figure 6.4. Particle average size was measured to be around 50 nm.

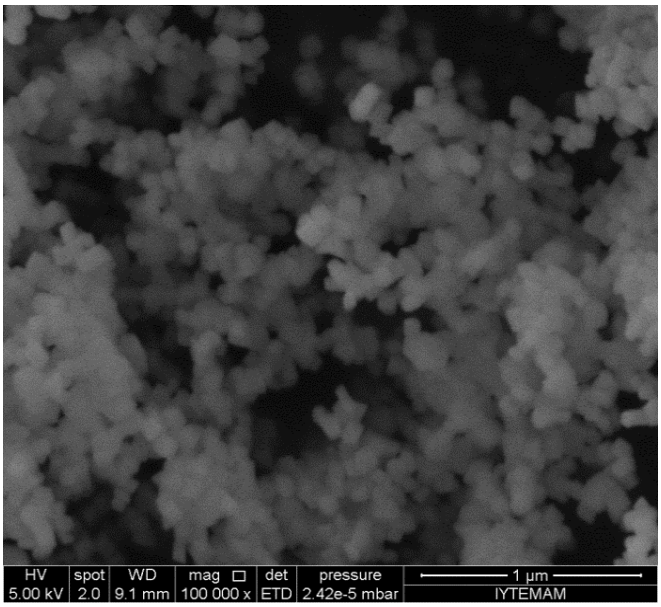

Figure 6.3. SEM image of CaCO3 (without surface treatment) (100000X magnification)

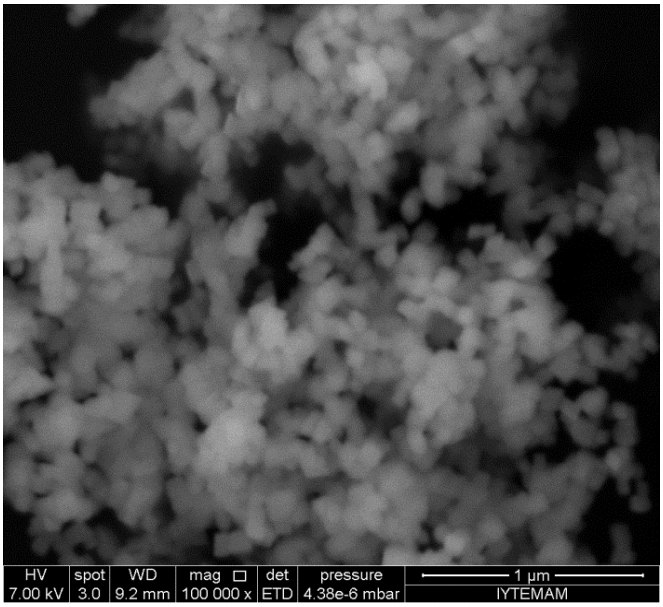

Figure 6.4. SEM image of $CaCO_3$ (with stearic acid surface treatment) (100000X magnification)

6.2. Polypropylene and Polyethylene Properties

6.2.1. Thermal Properties

6.2.1.1. Differential Scannig Calorimetry (DSC)

Figure 6.5 shows the DSC curves of neat PE and PP specimens. The melting temperature (T_m) of neat PP was 167^{o}C, while T_m of PE was 137^{o}C. The crystallization temperatures of neat PP and PE were 109^{o}C and 118^{o}C; respectively.

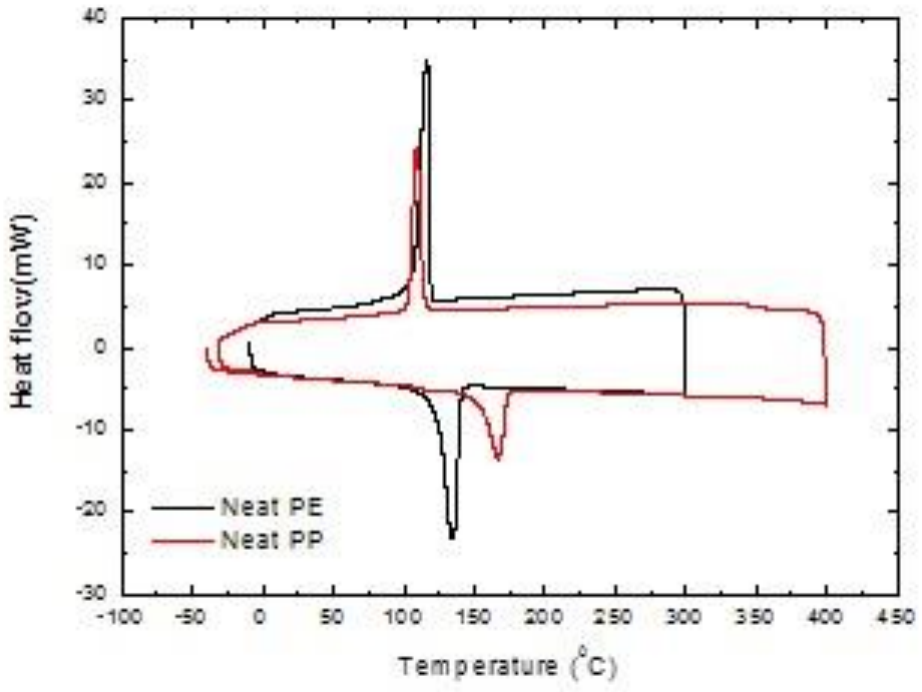

Figure 6.5. DSC curves of neat PE and PP specimens

6.2.1.2. Thermogravimetric Analysis (TGA)

Figure 6.6 shows TGA curve of the neat PE and PP specimens. The onset decomposition temperature of neat PP was lower value than that of neat PE. PP starts degrading about 280°C while PE starts degrading about 400°C. Maximum decomposition temperature for PP was about 450^{o}C while maximum decomposite

temperature for PE was about 510°C. Above 450°C and 510°C, for PP and PE respectively, no residue or char was visible.

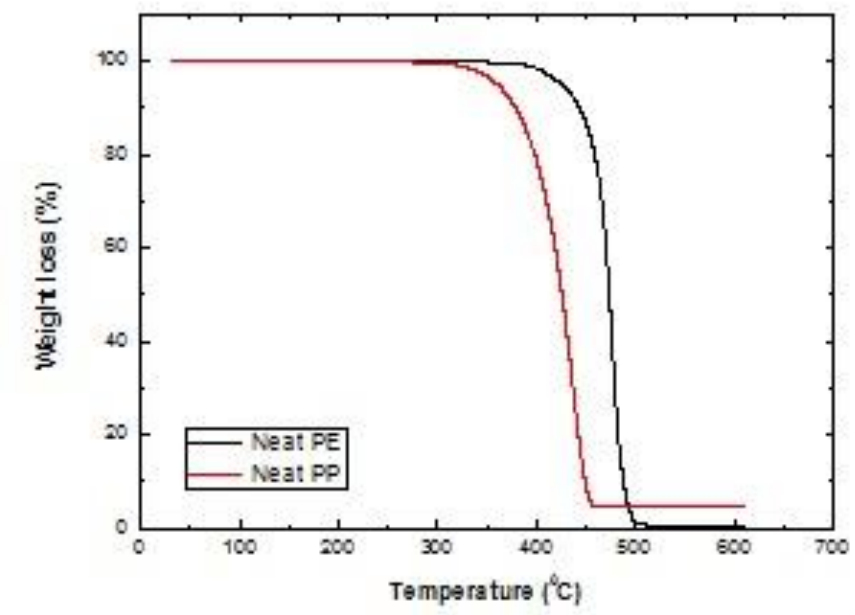

Figure 6.6. TGA curves of neat PE and PP specimens

6.3. $CaCO_3$ /Polypropylene Composite and Its Properties

6.3.1. Thermal Properties

6.3.1.1. Differential Scannig Calorimetry (DSC)

Figure 6.7 shows the DSC curves of $CaCO_3$ (without surface treatment)//PP composite specimens and Figure 6.8. shows the DSC curves of $CaCO_3$ (with stearic acid surface treatment)/PP composite specimens As seen in the figures, T_c peak value increased with the addition of calcite into the PP matrix but melting temperature was not changed. These results can be explained; with the addition of inorganic material into the system, particle surfaces were acting as a crystallization starting points during cooling and so T_c value increased but there was no change in melting temperature because it is depended on the material characteristic of polymeric materials.

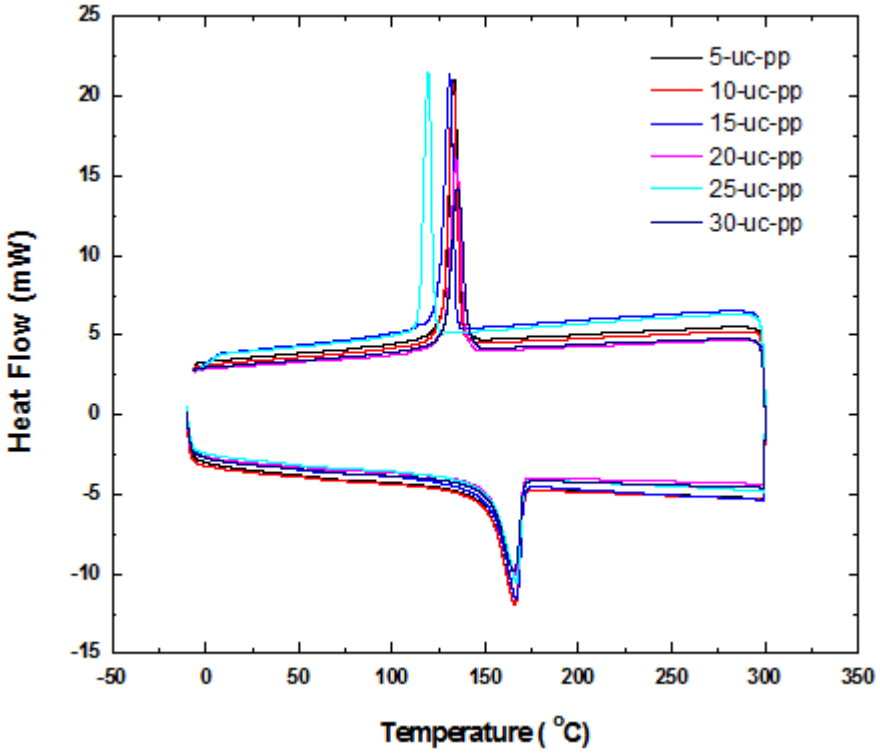

Figure 6.7. DSC curves of the $CaCO_3$ (without surface treatment)/PP composite specimens

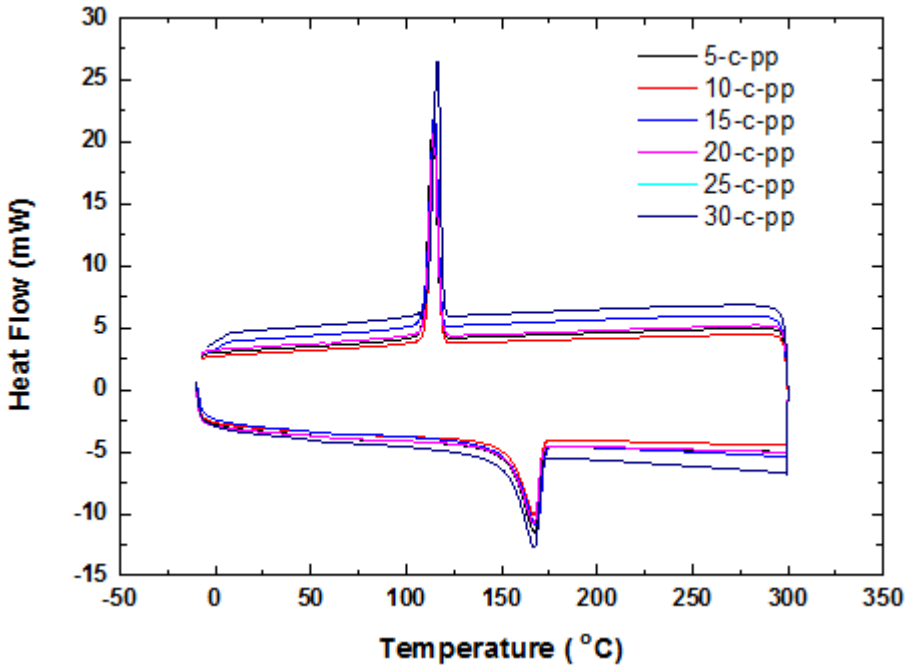

Figure 6.8. DSC curves of the $CaCO_3$(with stearic acid surface treatment)/PP composite specimens

6.3.1.2. Thermogravimetric Analysis (TGA)

Figure 6.9-6.10 shows the TGA curves of the $CaCO_3$(with and without surface treatment)/PP composite specimens. As seen in the figures, the initial decomposition temperature was shifted to higher value compared to neat PP. This confirmed the reinforcing effect of $CaCO_3$. $CaCO_3$ (uncoated)/PP composites degradation started around 330, and degradation rate was maximum around 420^{o}C. For $CaCO_3$ (coated)/PP composites degradation initiated around 370 ^{o}C, and degradation rate was maximum around 450 ^{o}C. At the end of degradation, both composite systems did not form measurable residue.

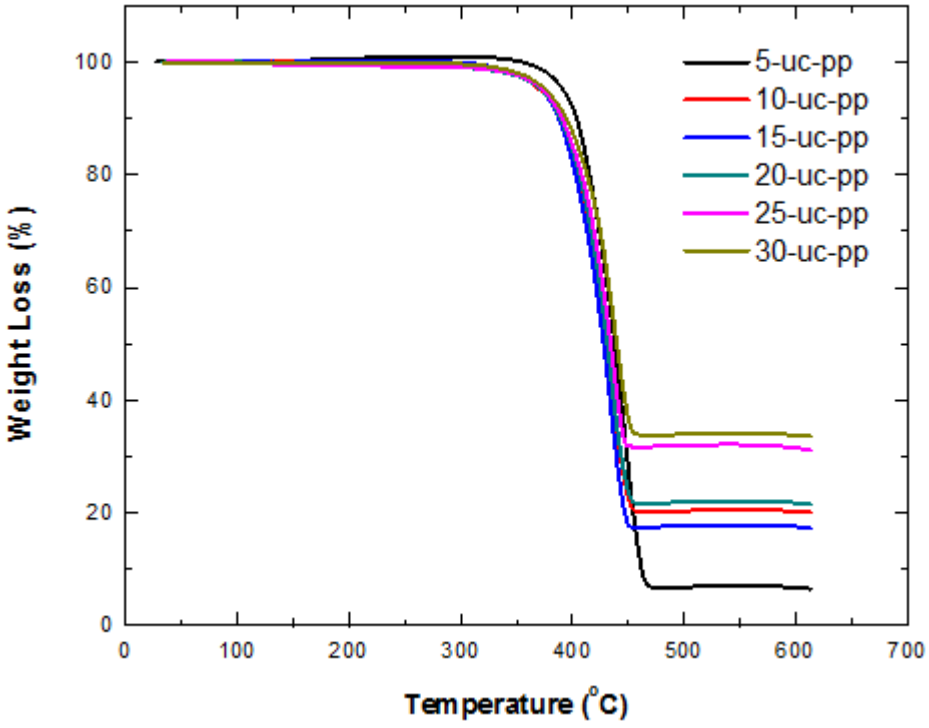

Figure 6. 9. TGA curves of $CaCO_3$ (without surface treatment)/PP composite specimens

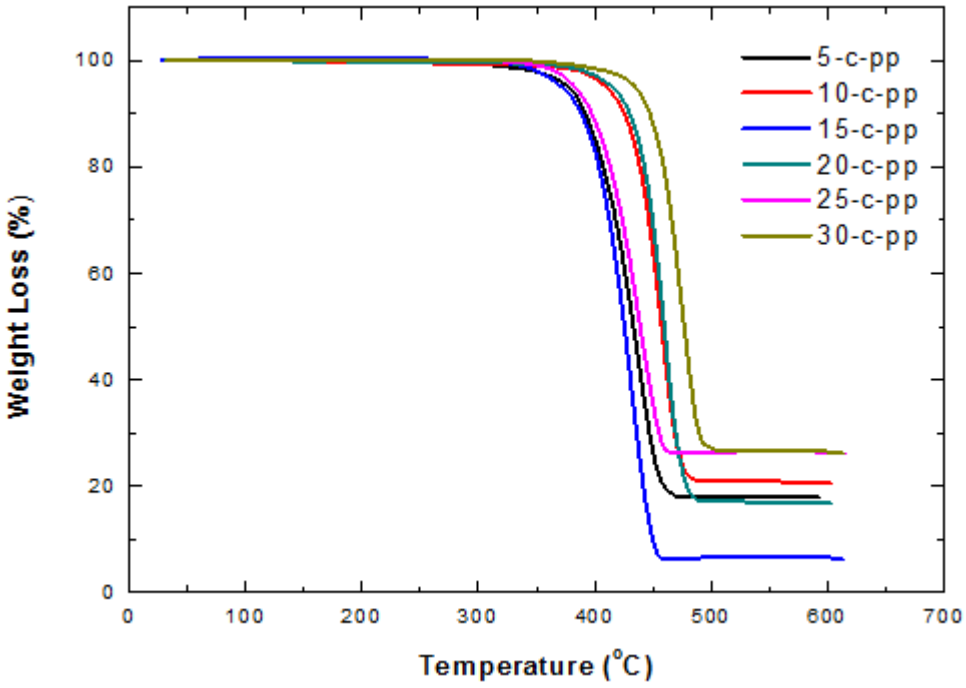

Figure 6.10. TGA curves of $CaCO_3$(with stearic acid surface treatment)/PP composite specimens

6.3.2. Mechanical Properties

6.3.2.1. Tensile Properties

Figure 6.11 shows the stress-strain curves of neat PP specimens. As seen in the figure, the initial curve was almost linear at low stresses and strains. After some displacement, the curve reached its maximum value (yield point). At this point, the necking was observed and it progressed stably along the specimen length and the test was stopped after the displacement reached to 150% deformation. The complete rupture was not observed for neat PP. Figures 6.12 and 6.13 shows stress-strain curves of calcite filled PP composites, respectively. The characteristics of these curves did not change significantly compared to those of neat PP. The yielding behavior was observed for neat PP and all calcite filled PP composite specimens. Brittle fracture was observed in high calcite content specimens. Additionally, the transformation from ductile to brittle was observed with the addition of calcite filler.

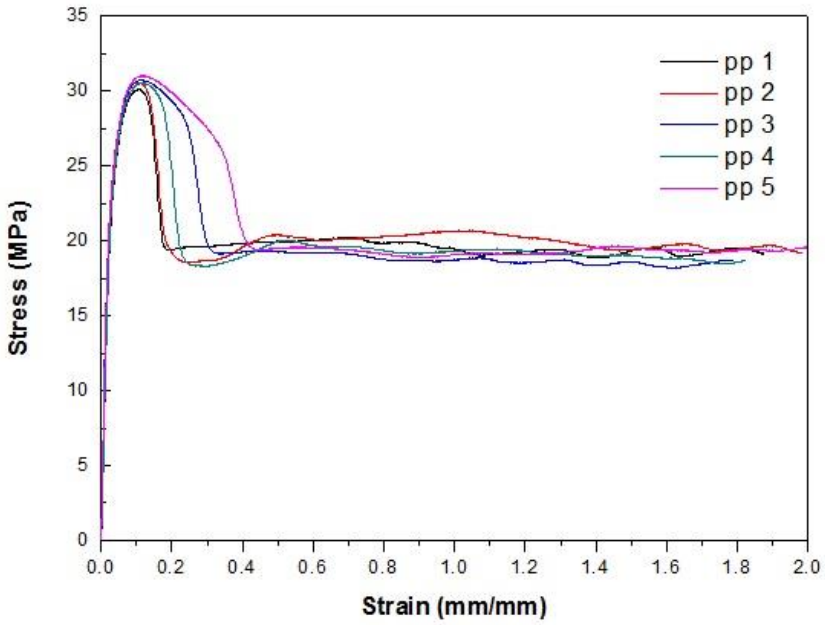

Figure 6.11. Stress-strain curves of neat PP

Figure 6.14. shows the effect of calcite content on the elastic modulus of composite specimens. As seen in the figure, elastic modulus increases with increasing the filler content. The elastic modulus of composite specimens reinforced with coated calcite were higher than those of specimens reinforced with uncoated calcite particles. The elastic modulus reaches to the maximum value when the filler content is 30 wt% for both uncoated/coated calcite particles.

Figure 6.15 shows the variation of yield strength of composite specimens with respect to filler content. As seen in the figure, the maximum yield strength was obtained when the filler content was 5 wt. % for both uncoated/coated particle filled specimens. Additionally, the filler content did not have a significant effect on the yield strength of composites.

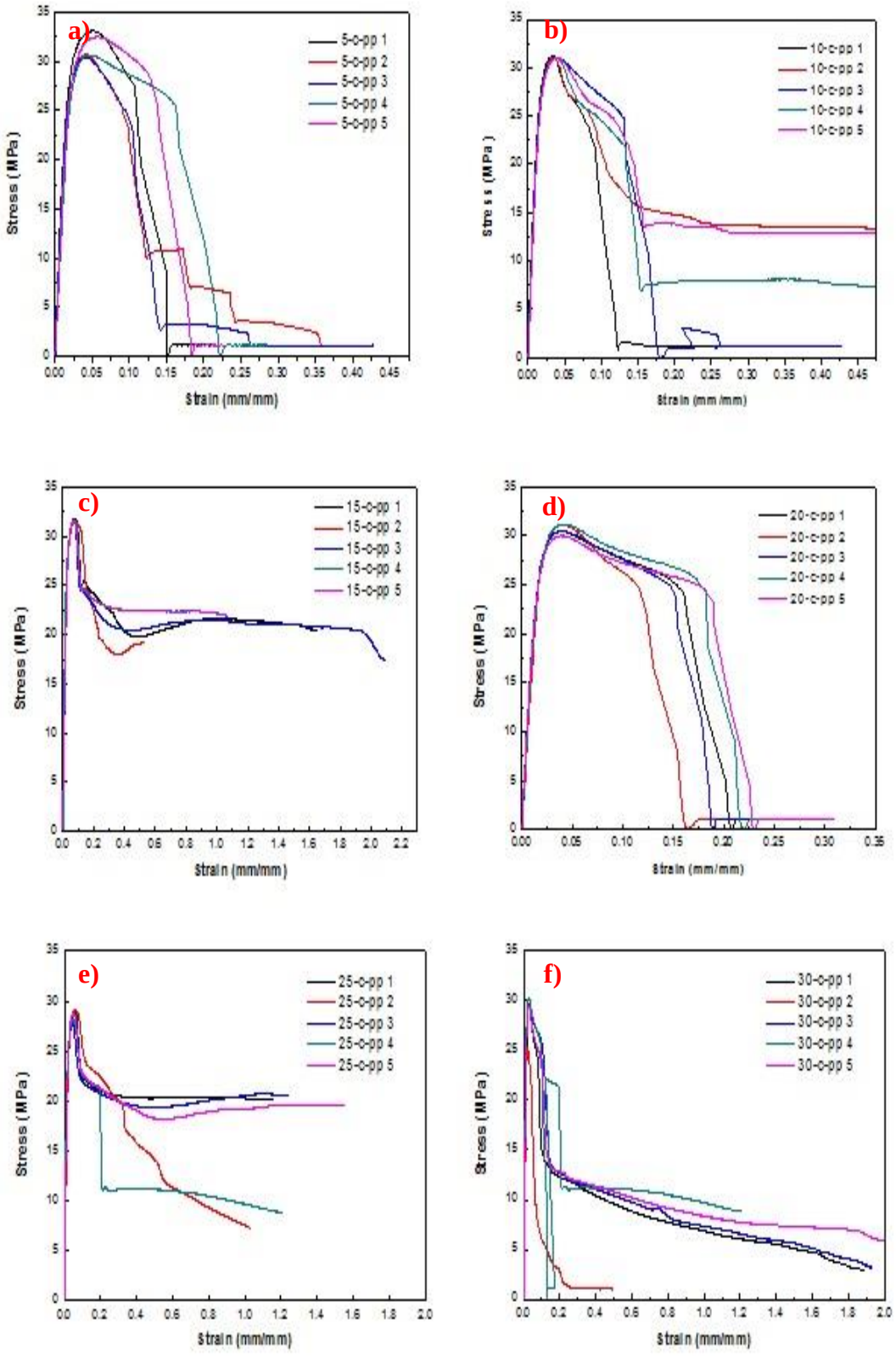

Figure 6.12. Stress-strain curves of the $CaCO_3$/PP specimens with different $CaCO_3$ (with stearic acid surface treatment) particle contents, (a) 5wt. %, (b) 10 wt. %, (c) 15 wt.%, (d) 20 wt. %, (e) 25 wt. %, (f) 30 wt. %

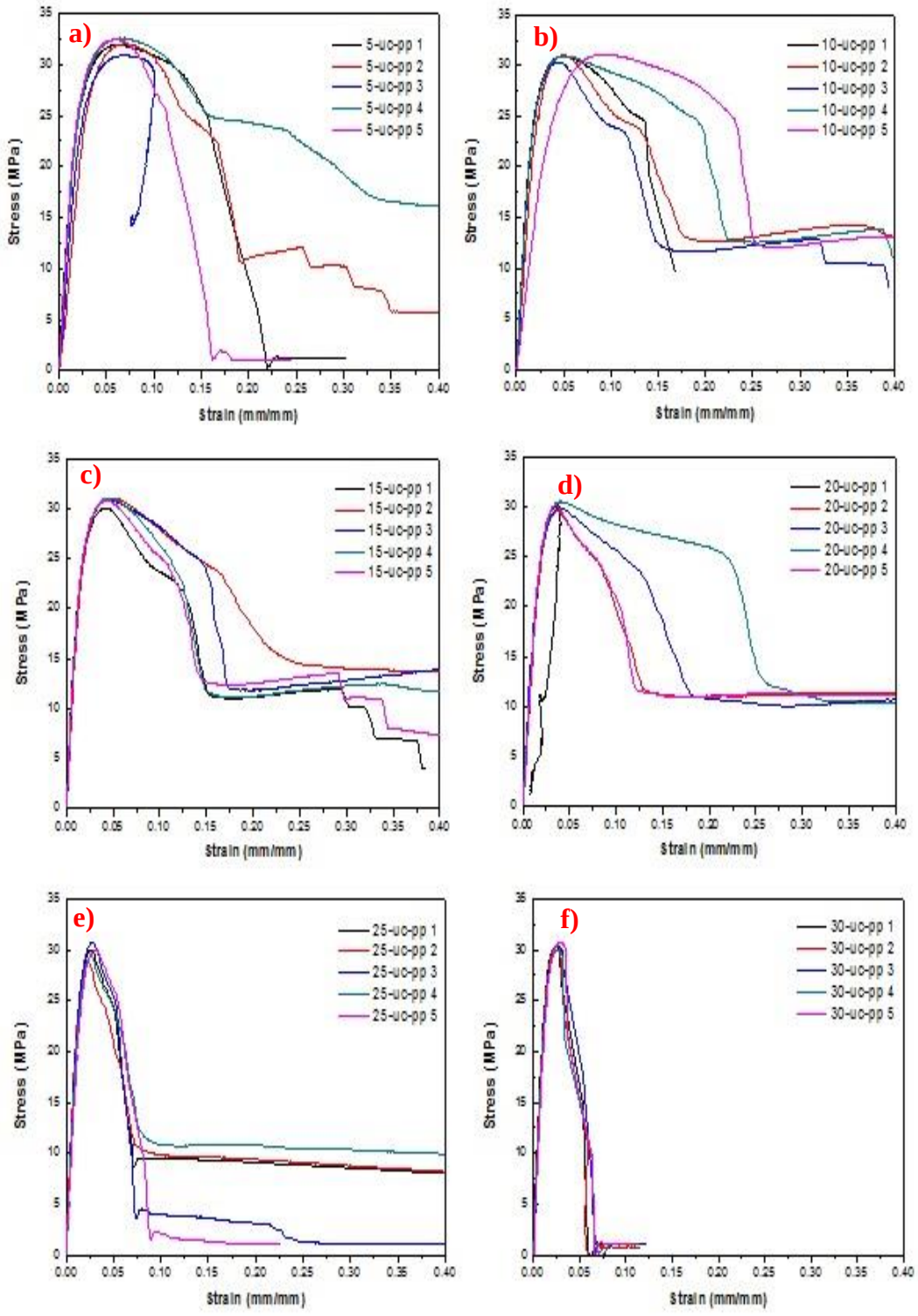

Figure 6.13. Stress-strain curves of the $CaCO_3$/PP specimens with different $CaCO_3$ (without surface treatment) particle contents, (a) 5wt. %, (b) 10 wt. %, (c) 15 wt.%, (d) 20 wt. %, (e) 25 wt. %, (f) 30 wt. %

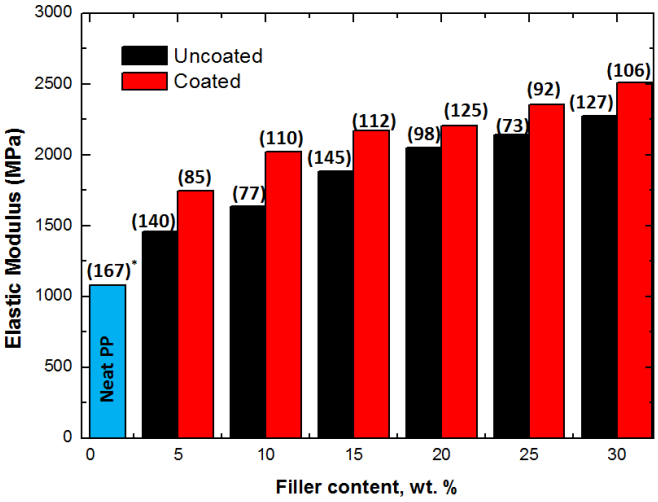

Figure 6.14. Elastic modulus of the $CaCO_3$/PP composite specimens as a function of filler content. *The values in parentheses ( ) represent the standard deviation for each test.

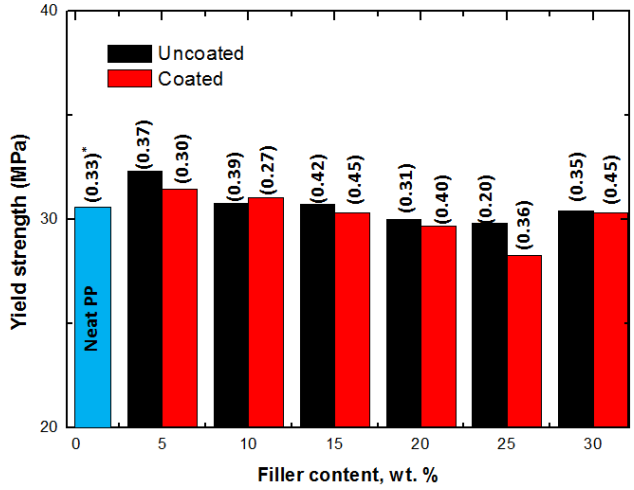

Figure 6.15. Yield strength of the $CaCO_3$/PP composite specimens as a function of filler content. *The values in parentheses ( ) represent the standard deviation for each test.

6.3.2.1.1. Analytical Calculations

The elastic modulus of $CaCO_3$/PP composites were calculated by using the law of mixtures equation:

$$E = E_p \phi_p + E_f \phi_f \tag{6.1}$$

where E_c is the modulus of the composites, E_p and E_f are the moduli of the polymer matrix and the filler, respectively, Φ_p and Φ_f are the volume fractions of the polymer and filler respectively. The elastic modulus of PP was taken as E=1.079 GPa from the experimental results. By using the Eq. (6.1), the modulus of nano-calcite was obtained as 24.60 GPa. This value corresponds well to measurements of the elastic modulus on the calcite in Ref. [23] where the value 26 GPa was obtained. Figure 6.16 shows the calculated (theoretical) and measured (experimental) moduli of $CaCO_3$/PP nanocomposites as a function of filler content. As seen in the figure, the experimental moduli of the nanocomposites agreed well with the theoretical values up till a filler content of 15 wt.%.

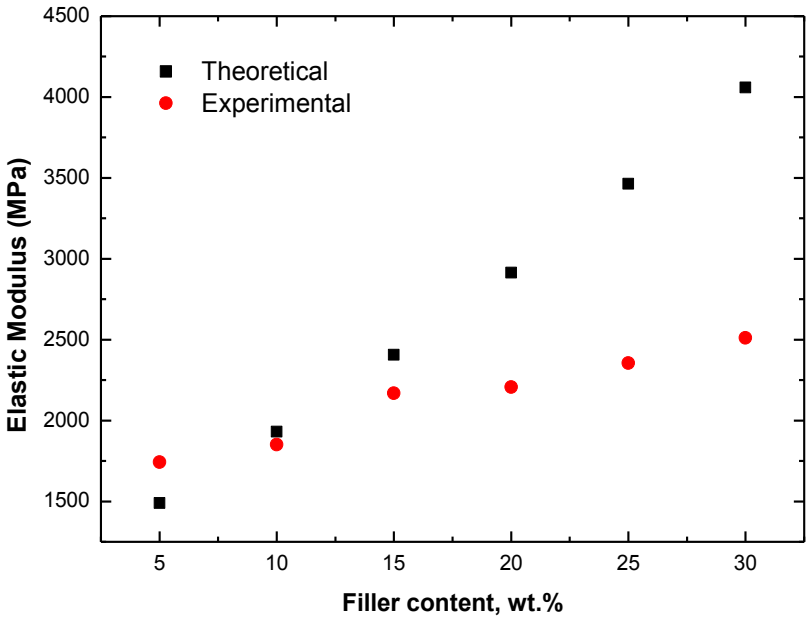

Figure 6.16. Comparison of the calculated (theoretical) and measured (experimental) moduli of $CaCO_3$/PP nanocomposites.

6.3.2.2. Flexural Properties

Figures 6.17 and 6.18 shows the variation of flexural modulus and strength with respect to $CaCO_3$ content; respectively. As seen in the figures, the values of flexural modulus and strength increases with the increase of $CaCO_3$ content. Maximum values was obtained at 30 wt. % filler content. The flexural modulus and strength values of specimens with uncoated $CaCO_3$ are higher than those of specimens with coated

$CaCO_3$. A drastic increase in flexural strength was observed when calcite content was 5wt. % for both uncoated/coated filled composites compared to neat PP. From 5% to 30 wt. % filler content, the flexural strength increases unsignificantly.

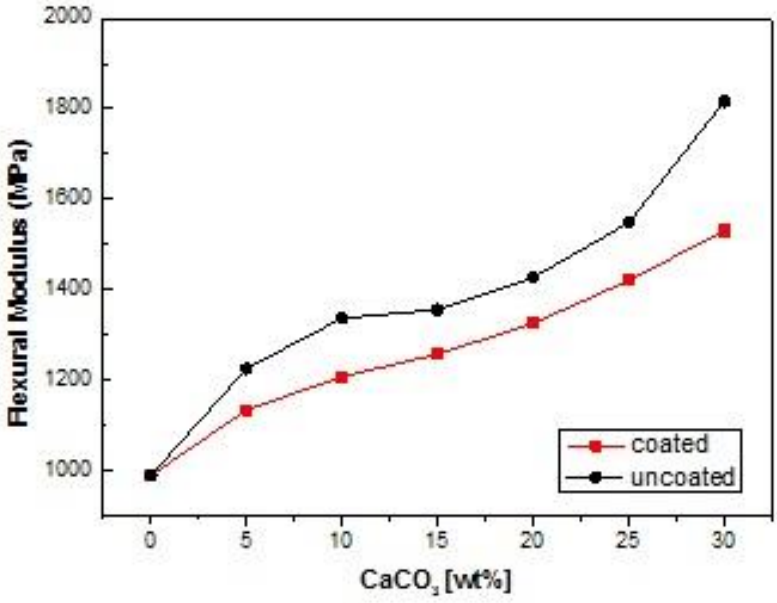

Figure 6.17. Flexural modulus of $CaCO_3$/PP composites as a function of $CaCO_3$ content

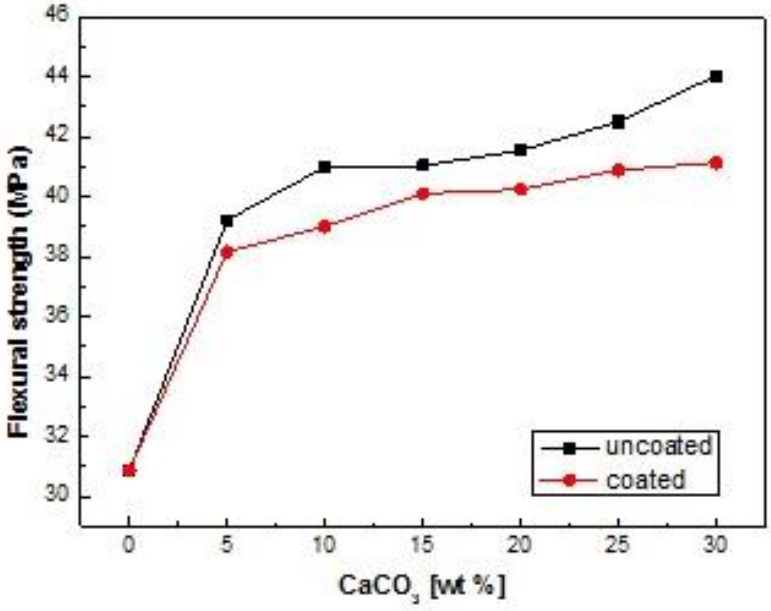

Figure 6.18. Flexural strength values of $CaCO_3$/PP composites as a function of $CaCO_3$ content

6.3.2.3. Impact Properties

Figure 6.19 shows the Charpy impact strength of $CaCO_3$/PP composites as a function of $CaCO_3$ content. As seen in the figure, the impact strength values of neat PP were higher than those of the $CaCO_3$/PP composite specimens. The addition of the calcite had a negative effect on the impact strength of neat PP. The impact strength of the specimens having 15 wt % calcite was close to the impact strength of neat PP. The impact strength of composite specimens containing coated calcite were higher than that of the uncoated particle filled composites.

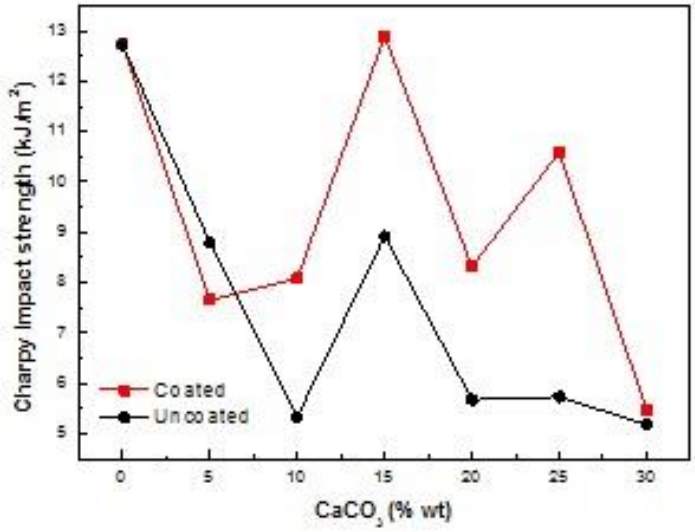

Figure 6.19. Charpy impact strength values of $CaCO_3$/PP composites as a function of $CaCO_3$ content

Figure 6.20 shows the SEM images of the fracture surface of neat PP specimens after the impact tests. Figures 6.21-6.24 shows the SEM images of $CaCO_3$/PP composites at filler contents of 5% and 30%, respectively. Microstructural analysis was performed on the fracture surfaces by using the SEM technique. The aim of this analysis is to examine the effect of calcite on the microstructure of the PP composites which were prepared in the twin-screw extruder. In the SEM micrographs of these materials, the calcium carbonate particles in nano dimension and their dispersion can be clearly seen. The uncotated $CaCO_3$ particles were dispersed in the matrix irregularly, and some big aggregates were observed on the fracture surface (Figure 6.21 and 6.23). The SEM

images of the composites with $CaCO_3$ particles with stearic acid surface treatment have small agglomerate (Figure 6.22 and 6.24).

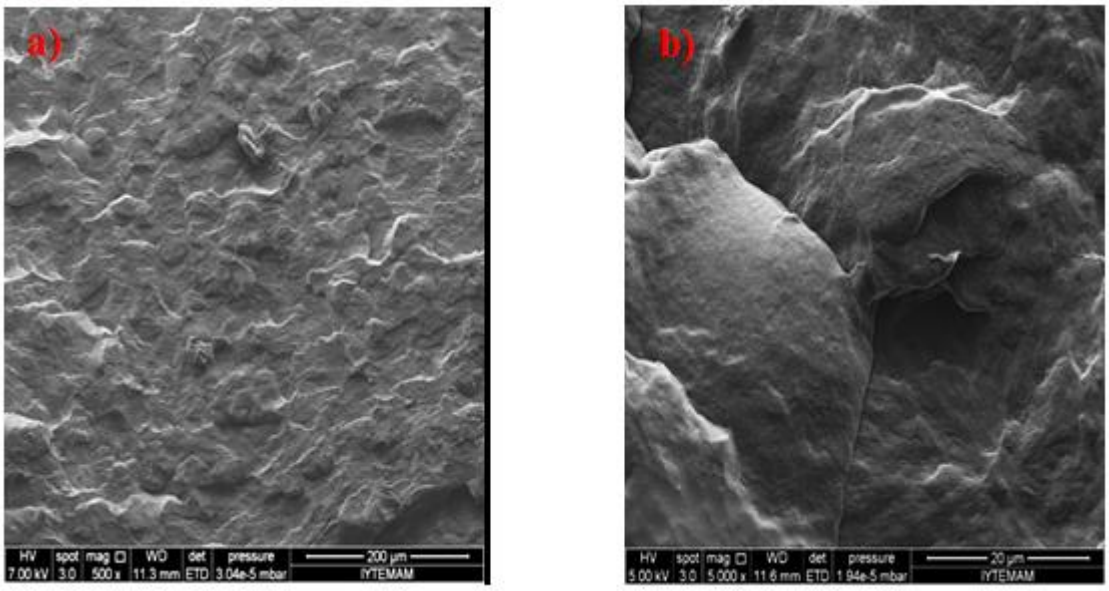

Figure 6.20. SEM images of the impact fractured surface of neat polypropylene, (a) 500X magnification, (b) 5000X magnification

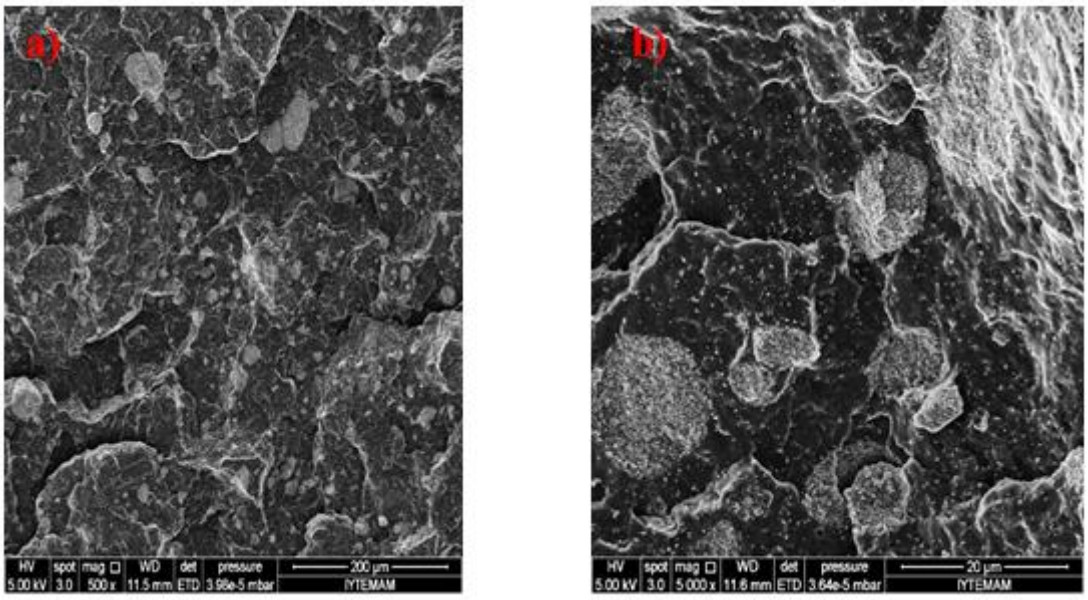

Figure 6.21. SEM images of the impact fractured surface of 5 wt. % $CaCO_3$ (uncoated) filled polypropylene, (a) 500X magnification, (b) 5000X magnification

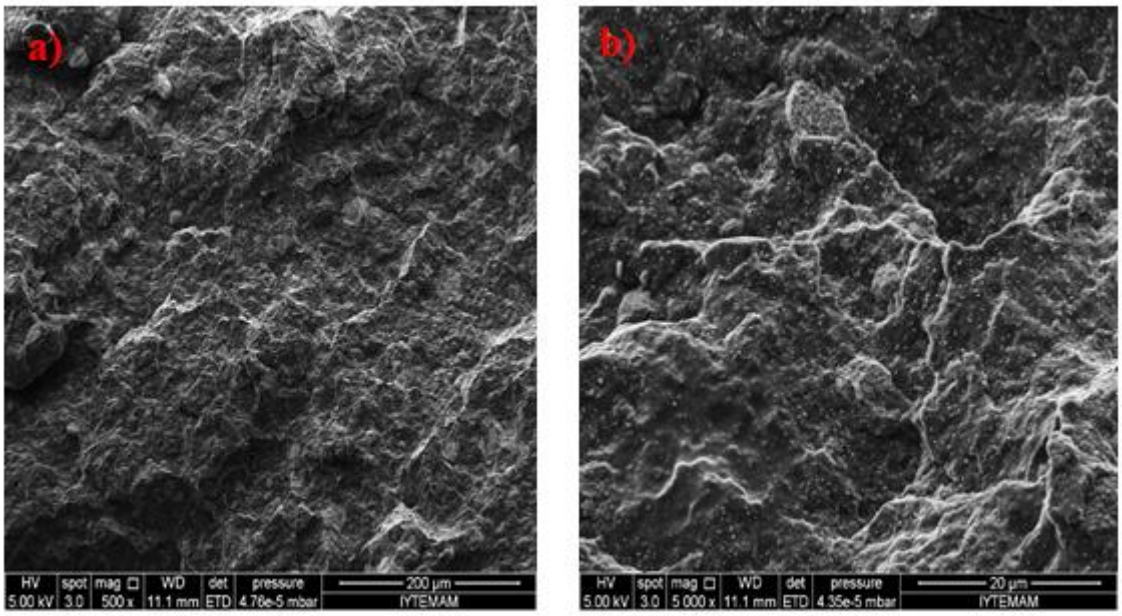

Figure 6.22. SEM images of the impact fractured surface of 5 wt. % $CaCO_3$ (coated) filled polypropylene, (a) 500X magnification, (b) 5000X magnification

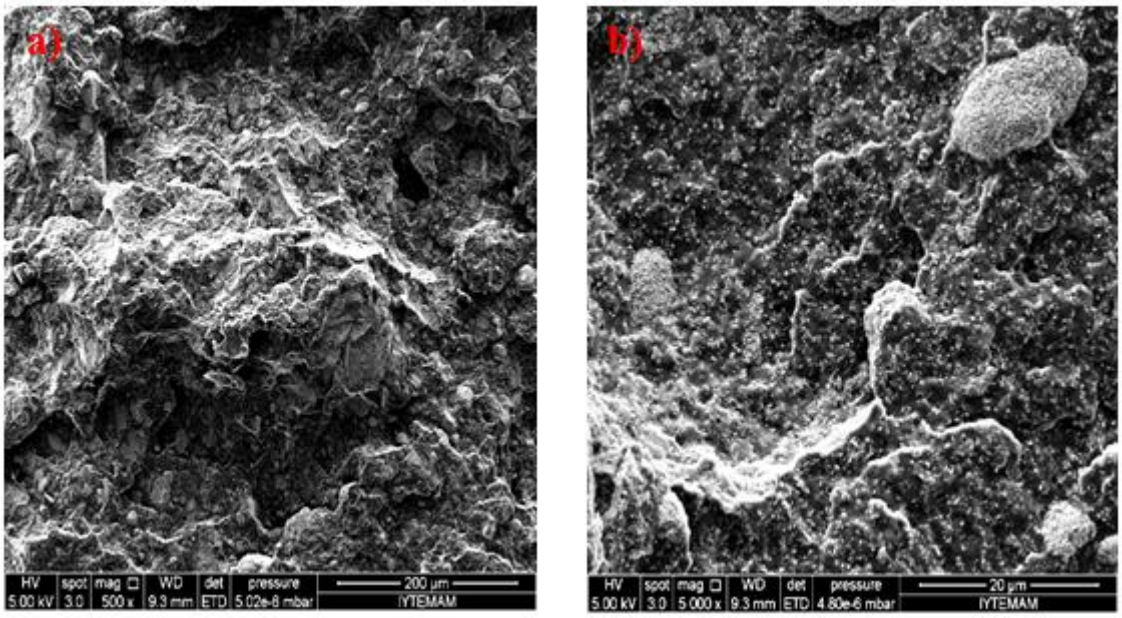

Figure 6.23.SEM images of the impact fractured surface of 30 wt. % $CaCO_3$ (uncoated) filled polypropylene, (a) 500X magnification, (b) 5000X magnification

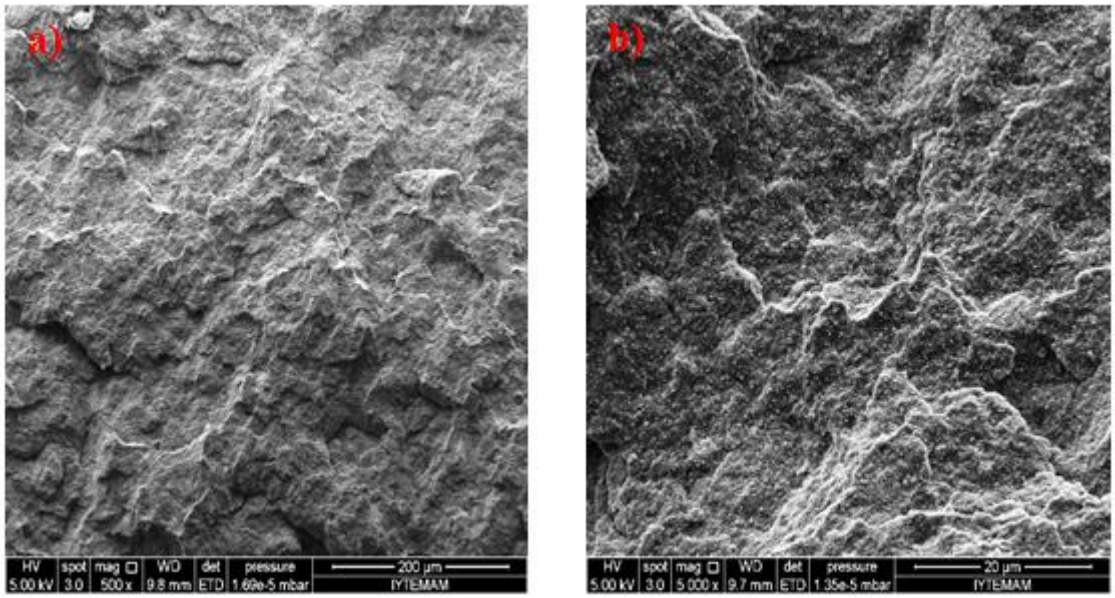

Figure 6.24. SEM images of the impact fractured surface of 30 wt. % $CaCO_3$ (coated) filled polypropylene, (a) 500X magnification, (b) 5000X magnification

6.4. $CaCO_3$ / Polyethylene Composite and Its Properties

6.4.1. Thermal Properties

6.4.1.1. Differential Scanning Calorimetry (DSC)

Figure 6.25-6.26 shows the DSC curves of the $CaCO_3$/PE composite specimens. As seen in the figures, the effect of calcite addition on the melting temperature was insignificant. T_c values increased with the addition of calcite into the PE matrix. This effect was more observable for coated specimens. These results suggest that; with the addition of inorganic material in to the system, particle surfaces were acting as a crystallization starting points during cooling and so T_c value decreased but there was no change in melting temperature because it is depended on the material characteristic of polymeric materials.

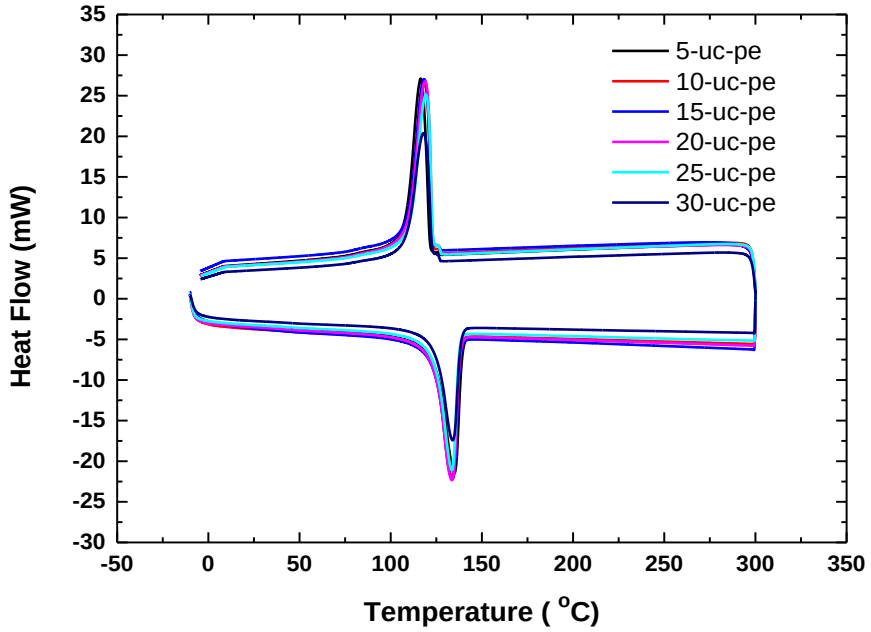

Figure 6.25. DSC curves of the $CaCO_3$ (without surface treatment)/PE composite specimens

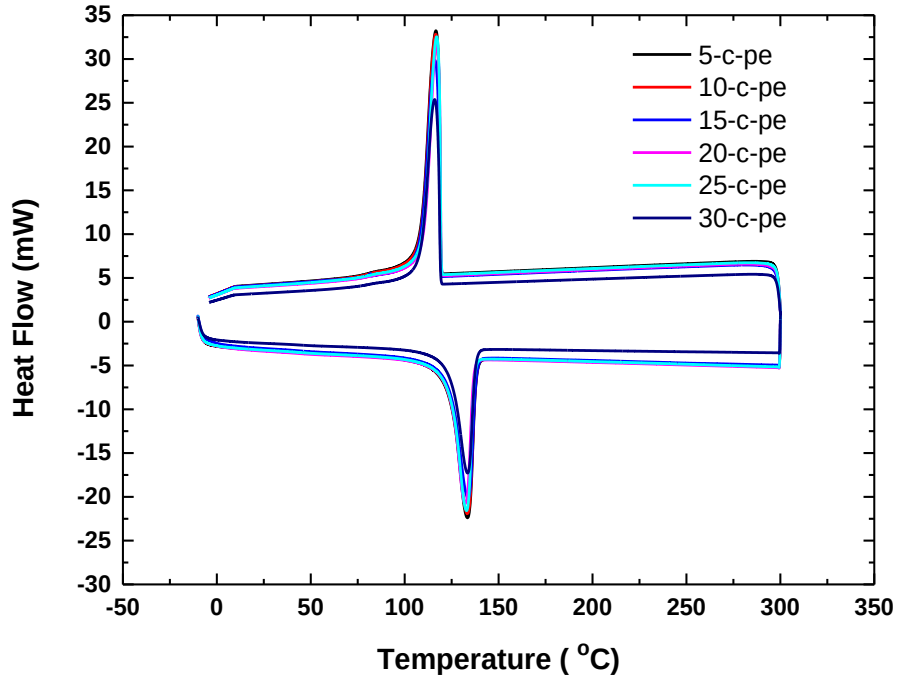

Figure 6.26. DSC curves of the $CaCO_3$ (with stearic acid surface treatment)/PE composite specimens

6.4.1.2. Thermogravimetric Analysis (TGA)

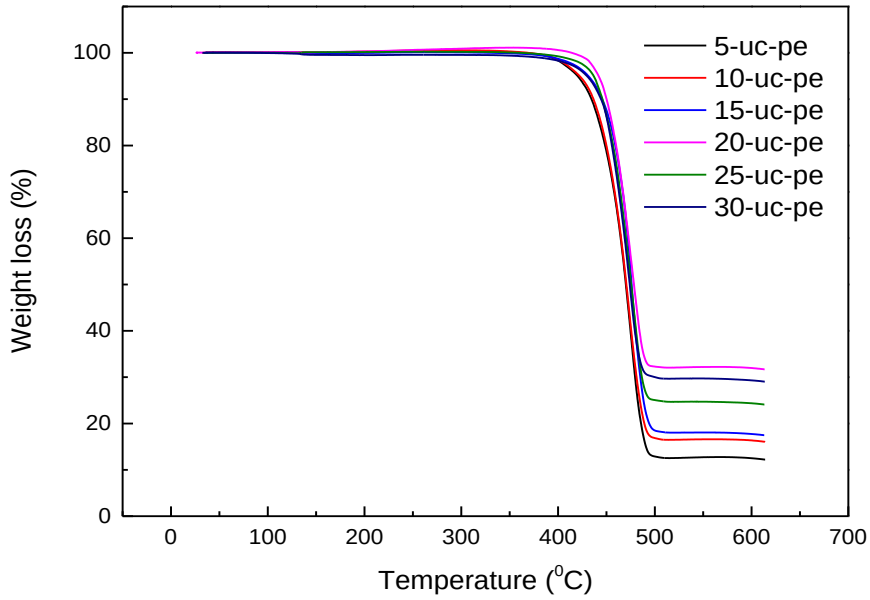

Figure 6.27. TGA curves of the $CaCO_3$ (without surface treatment)/PE composite specimens

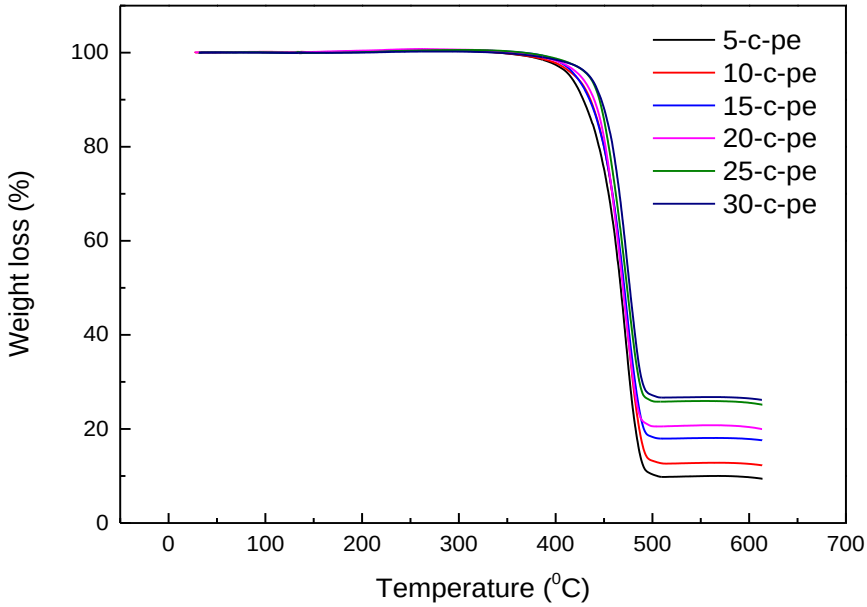

Figure 6.28. TGA curves of the $CaCO_3$ (with stearic acid surface treatment)/PE composite specimens

Figure 6.27-6.28. shows the TGA curves of the $CaCO_3$/PE composite specimens. The reinforcing effect of $CaCO_3$ was still observable as in case of $CaCO_3$/PP composites. The initial decomposition temperature of the uncoated $CaCO_3$/PE composites was about 370^oC, for coated $CaCO_3$/PE composites was 390^oC. Degradation rate was maximum around 500^oC for both uncoated/coated $CaCO_3$/PE composite specimens. At the end of degradation both composite systems did not form measurable residue.

6.4.2. Mechanical Properties

6.4.2.1. Tensile Properties

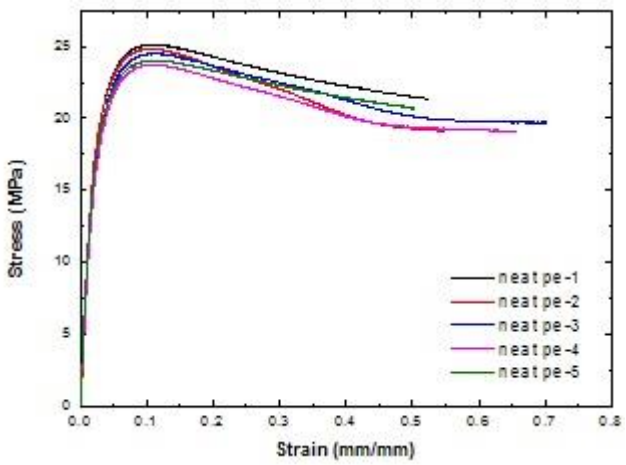

Figure 6.29. Stress-strain curves of neat PE

Figure 6.29 shows the stress-strain curves of neat PE specimens. As seen in the figure, the initial curve was almost linear at low stresses and strains. After some displacement, the curve reached its maximum value (yield point). At this point, the necking was observed and it progressed stably along the specimen length and the test was stopped after the displacement reached to 50% elongation. The complete rupture was not observed for neat PP.

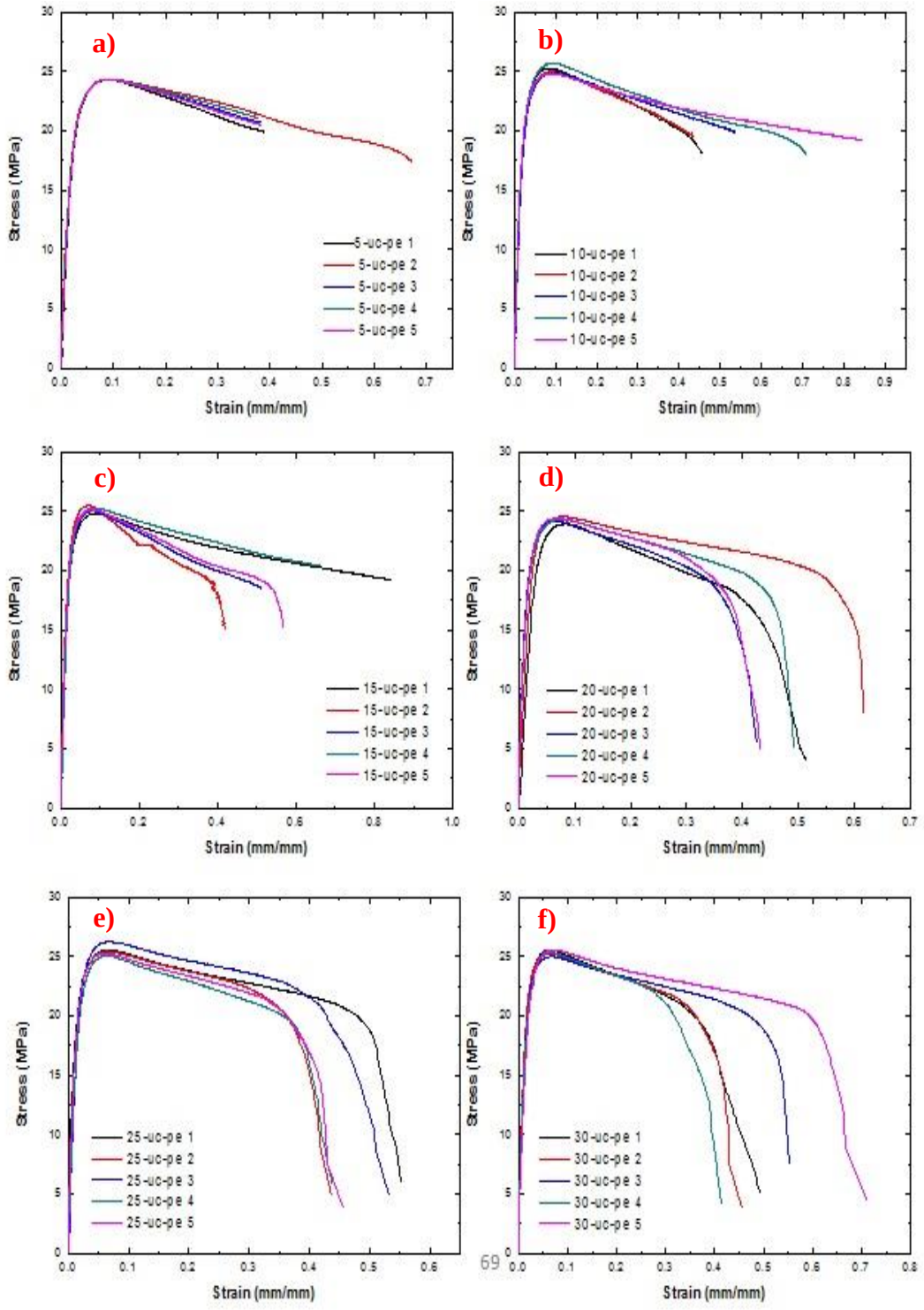

Figure 6.30. Stress-strain curves of the $CaCO_3$/PE specimens with different $CaCO_3$ (without surface treatment) particle contents, (a) 5wt. %, (b) 10 wt. %, (c) 15 wt.%, (d) 20 wt. %, (e) 25 wt. %, (f) 30 wt. %

Figures 6.30-6.31. shows the stress-strain curves of calcite filled PE composites. The characteristics of these curves did not change significantly compared to neat PE.

The yielding behavior was observed for neat PE and all calcite filled PE composite specimens.

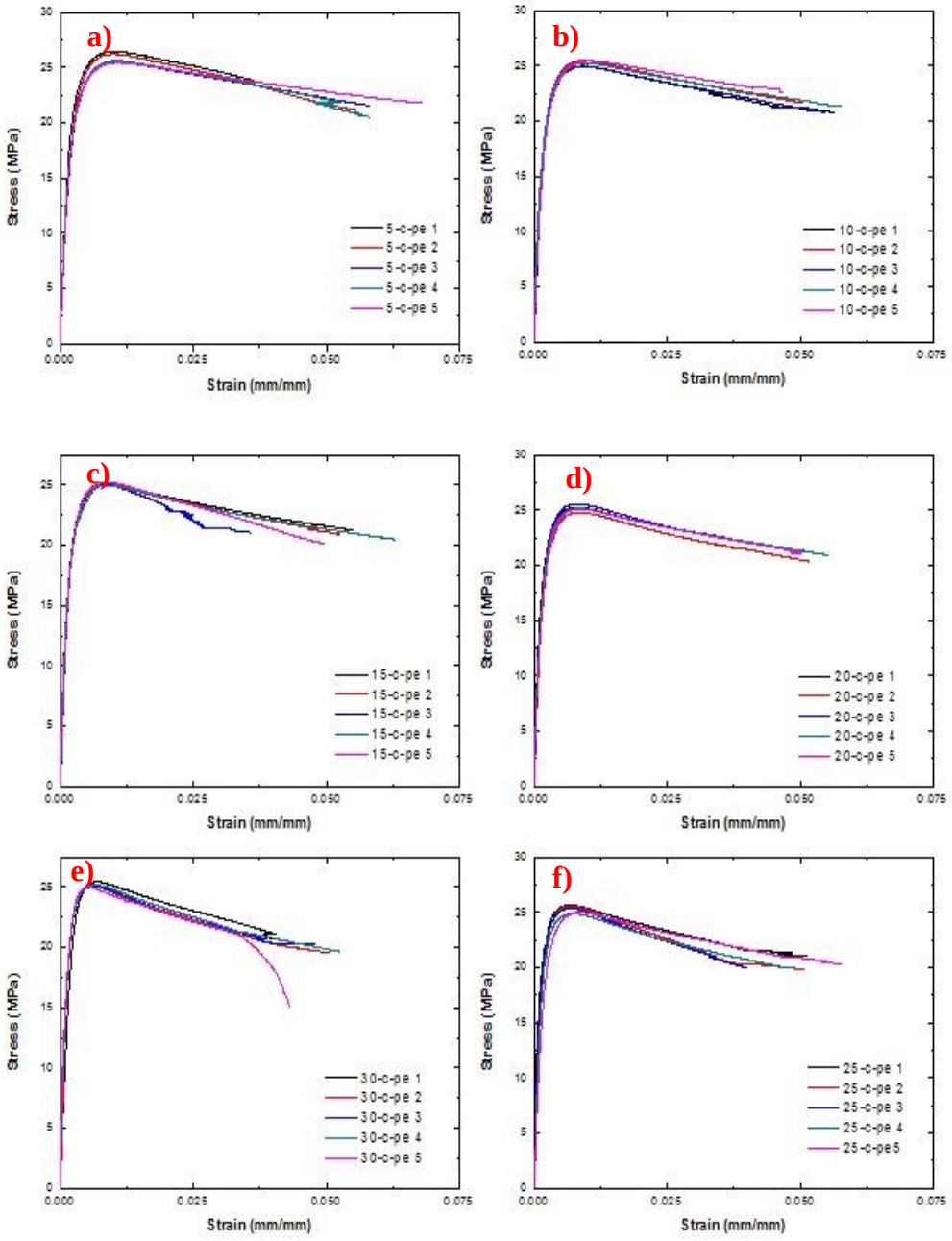

Figure 6.31. Stress-strain curves of the $CaCO_3$/PE specimens with different $CaCO_3$ (without surface treatment) particle contents, (a) 5wt. %, (b) 10 wt. %, (c) 15 wt.%, (d) 20 wt. %, (e) 25 wt. %, (f) 30 wt. %

Figure 6.32 shows the effect of calcite content on the elastic modulus of $CaCO_3$/PE composite specimens. As seen in the figure, elastic modulus increases as the filler content increases. The elastic modulus of composite specimens reinforced with

coated calcite were higher than those of specimens reinforced with uncoated calcite. The elastic modulus reaches to the maximum value when the filler content is 30 wt% for both uncoated/coated calcite.

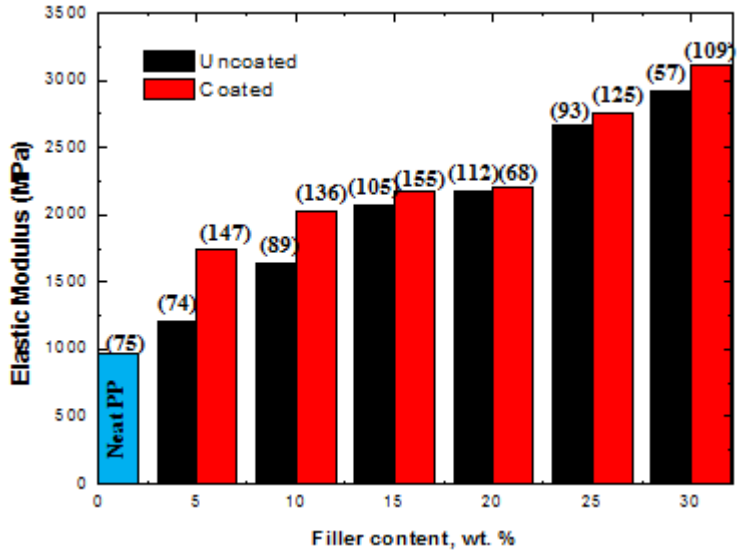

Figure 6.32. Elastic modulus of the $CaCO_3$/PE composite specimens as a function of filler content. *The values in parentheses ( ) represent the standard deviation for each test.

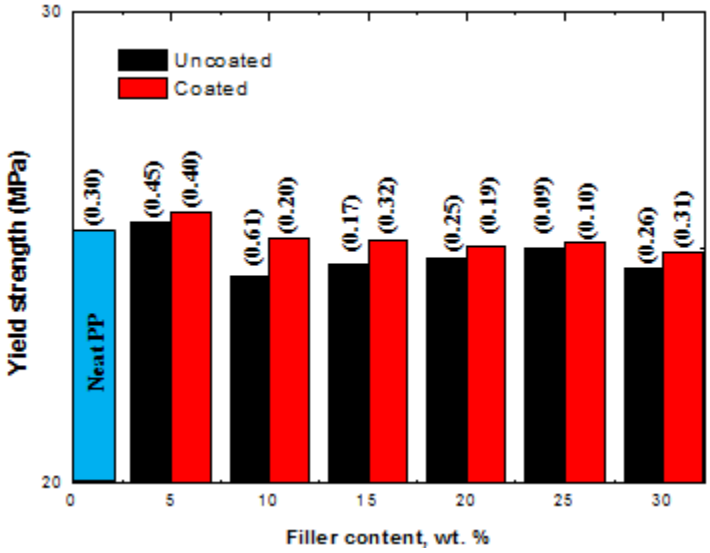

Figure 6.33. Yield strength of the $CaCO_3$/PE composite specimens as a function of filler content. *The values in parentheses ( ) represent the standard deviation for each test.

Figure 6.33 shows the variation of yield strength of $CaCO_3$/PE composite specimens with respect to filler content. As seen in the figure, the maximum yield strength was obtained when the filler content was 5 wt. % for both uncoated/coated particle filled specimens. Additionally, the filler content did not have a significant effect on the yield strength of composites.

6.4.2.1.1. Analytical Calculations

The elastic modulus of $CaCO_3$/PE composites were calculated by using Eq. (6.1). The elastic modulus of neat PE and calcite were taken as E=0.960 GPa and E=24.60 GPa; respectively. Figure 6.34 shows the calculated (theoretical) and measured (experimental) moduli of $CaCO_3$/PE nanocomposites as a function of filler content. As seen in the figure, the experimental moduli of the nanocomposites is consistent with the theoretical values up till a filler content of 15 wt.%.

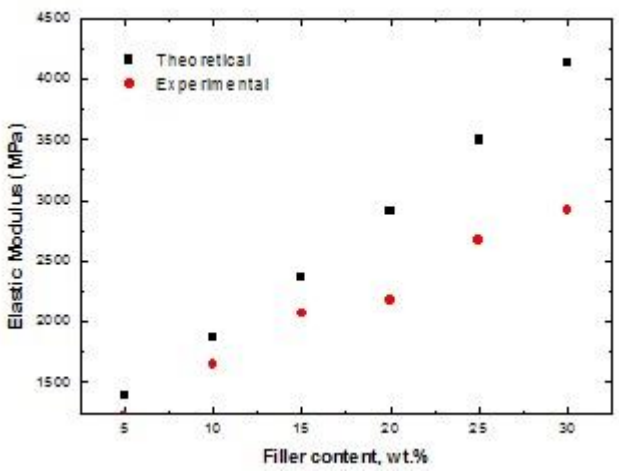

Figure 6.34. Comparison of the calculated (theoretical) and measured (experimental) moduli of $CaCO_3$/PE nanocomposites

6.4.2.2. Flexural Properties

Figure 6.35 shows the flexural modulus as a function of $CaCO_3$ content. As seen in the figure, the flexural modulus increased as the filler content increased. Up to 15 wt. % filler content, the flexural modulus of composite specimens with uncoated filler was higher than those of the composite specimens with coated filler. At higher filler content

(30 wt. %), the flexural modulus reaches to the maximum value when the coated calcite filler was used.

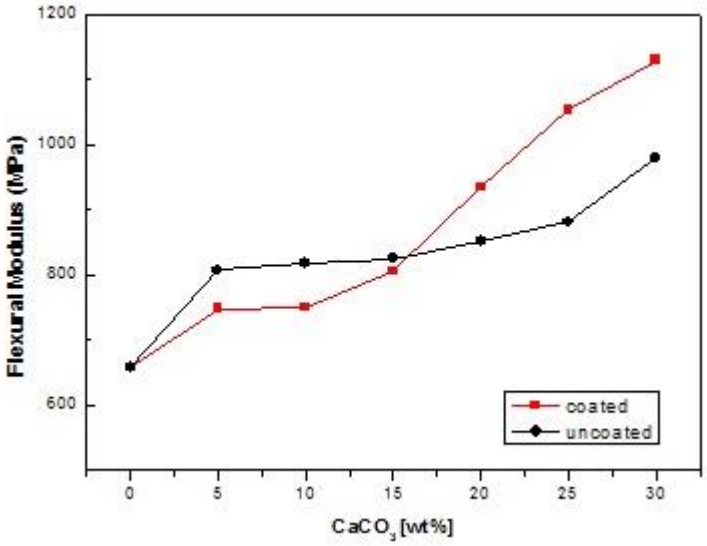

Figure 6.35. Flexural modulus of $CaCO_3$/PE composites as a function of $CaCO_3$ content

Figure 6.36 shows the flexural strength as a function of $CaCO_3$ content. As seen in the figure, flexural strength increased as the filler content increased. Up to 15 wt. % filler content, the flexural strength of composite specimens with coated filler was higher than those of composite specimens with uncoated filler. At higher filler content (30 wt. %), the flexural modulus took its maximum value when the uncoated calcite filler was used.

6.4.2.3. Impact Properties

Figure 6.37 shows the Charpy impact strength values of $CaCO_3$/PE composites as a function of $CaCO_3$ content. As seen in the figure, the impact strength values of neat PE were higher than those of the $CaCO_3$/PE composite specimens. The addition of the calcite had a negative effect on the impact strength of neat PE. The impact strength of composite specimens containing coated calcite were higher than uncoated composites except for 20 wt. %..

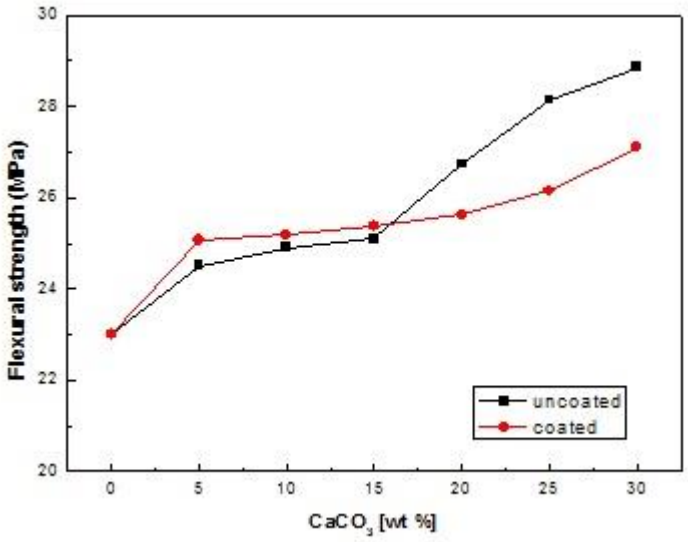

Figure 6.36. Flexural strength values of $CaCO_3$/PE composites as a function of $CaCO_3$ content

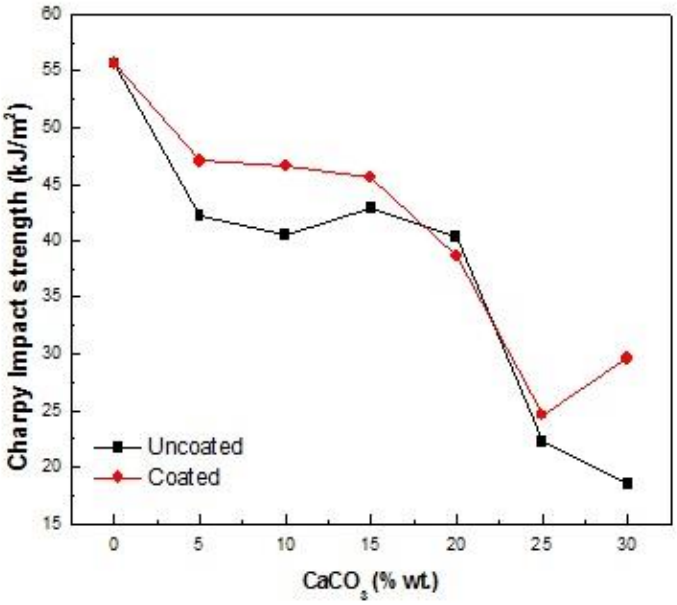

Figure 6.37. Charpy impact strength values as a function of $CaCO_3$ content

Figures 6.38 presents the SEM images of the impact fracture surface of neat PE, and Figures 6.39-6.42 shows the SEM images of the impact fracture surfaces of $CaCO_3$/PE composite specimens with a particle content of 5 and 30 wt.% for both uncoated and coated fillers. The uncoated $CaCO_3$ particles were dispersed in the matrix of PE irregularly (Figure 6.39 and 6.41).

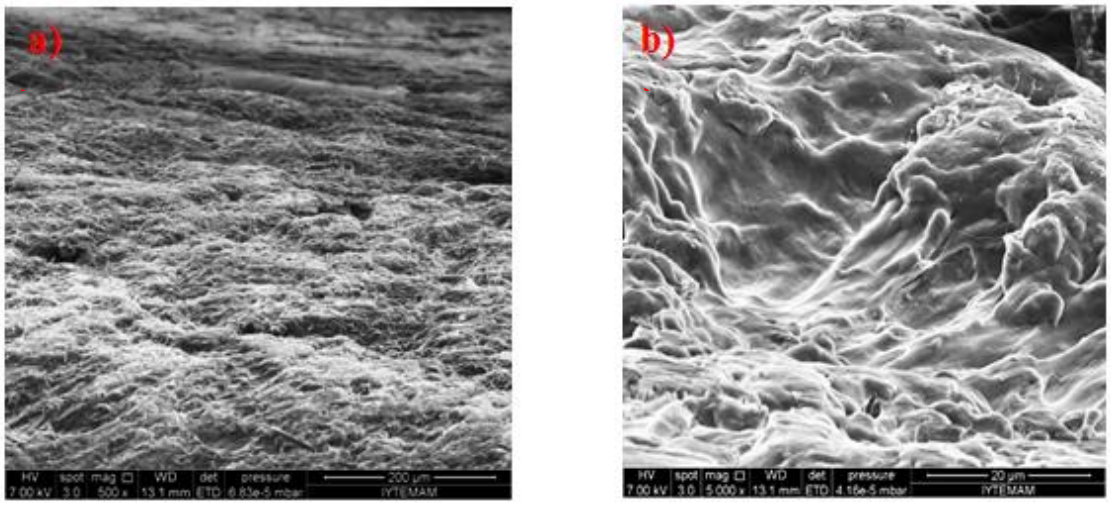

Figure 6.38. SEM images of the impact fractured surface of neat polyethylene, (a) 500X magnification, (b) 5000X magnification

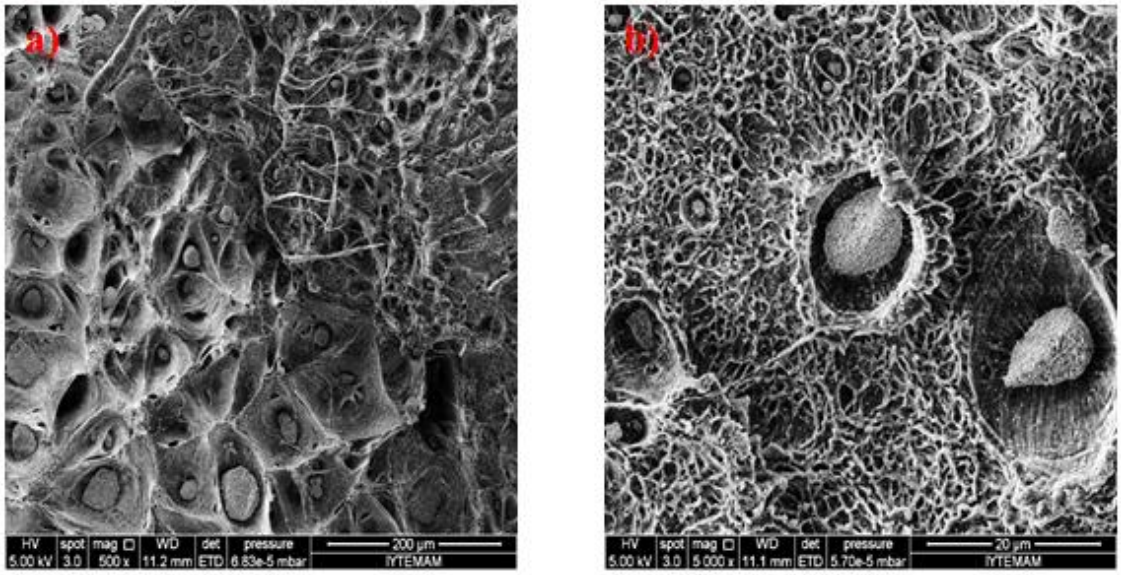

Figure 6.39. SEM images of the impact fractured surface of 5 wt. % $CaCO_3$ (uncoated) filled polyethylene, (a) 500X magnification, (b) 5000X magnification

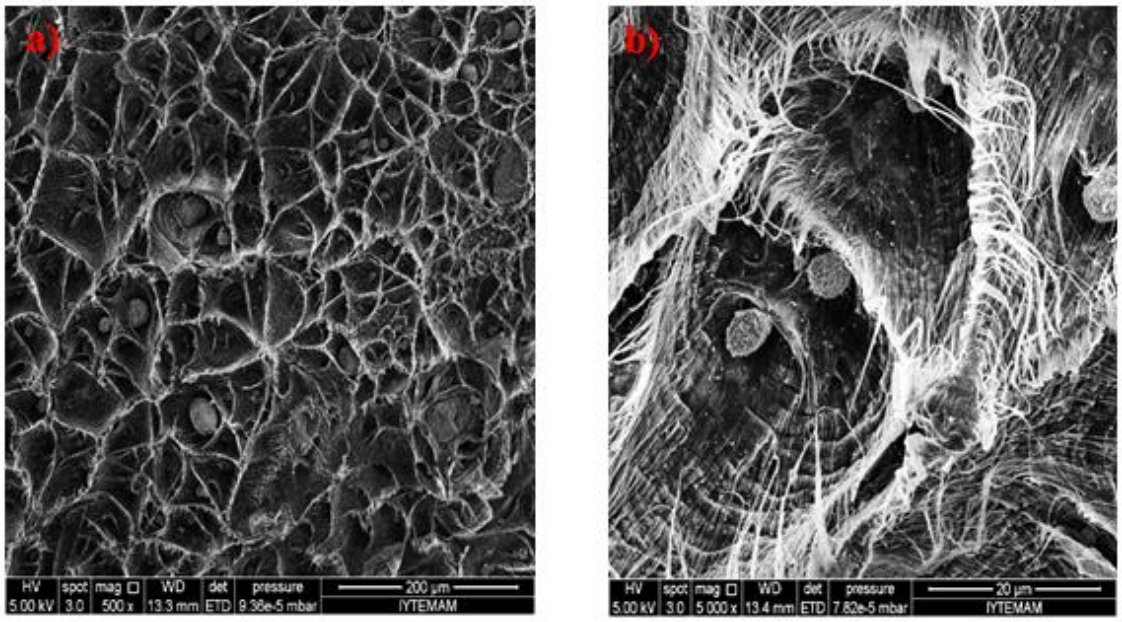

Figure 6.40. SEM images of the impact fractured surface of 5 wt. % $CaCO_3$(coated) filled polyethylene, (a) 500X magnification, (b) 5000X magnification

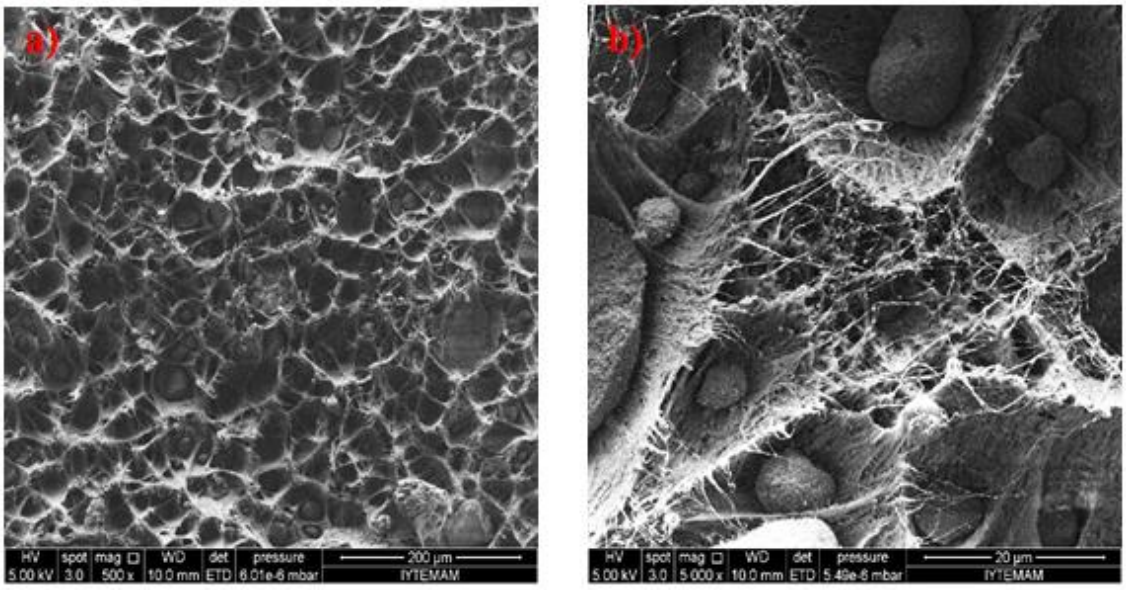

Figure 6.41. SEM images of the impact fractured surface of 30 wt. % $CaCO_3$ (uncoated) filled polyethylene, (a) 500X magnification, (b) 5000X magnification

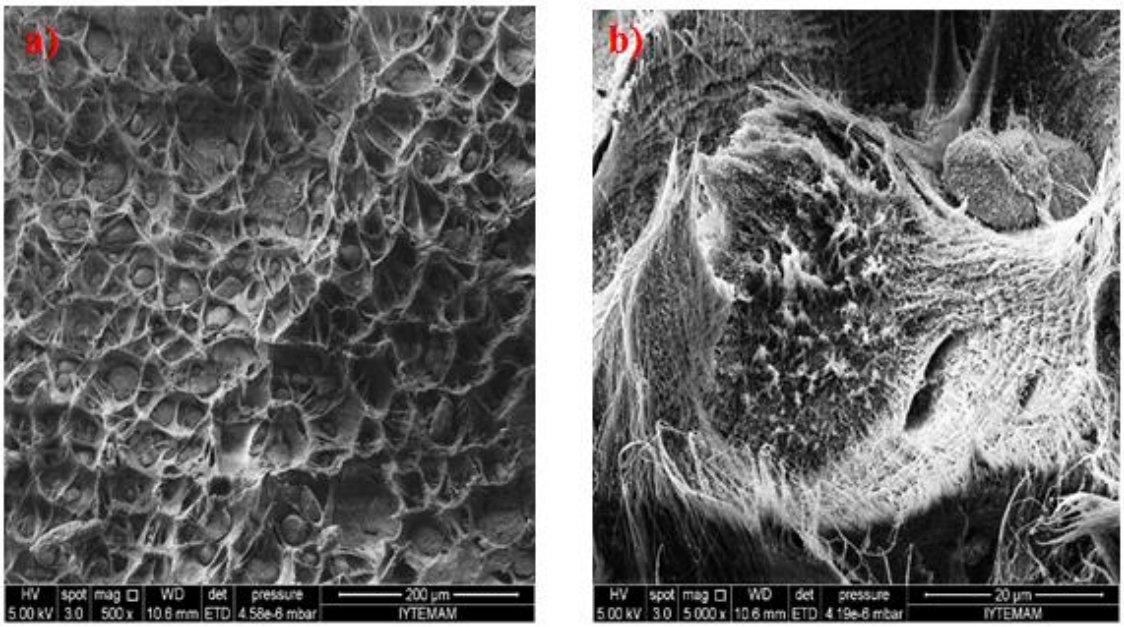

Figure 6.42. SEM images of the impact fractured surface of 30 wt. % $CaCO_3$ (coated) filled polyethylene, (a) 500X magnification, (b) 5000X magnification

CHAPTER 7

CONCLUSIONS

In this study, the effects of $CaCO_3$ particles (with and without stearic acid surface treatment), mixing conditions on the microstructural, thermal and mechanical behavior of $CaCO_3$/PP and $CaCO_3$/PE composites were investigated. $CaCO_3$/PP and $CaCO_3$/PE composite blends were prepared using co-rotational twin screw extruder with different particle contents (5, 10, 15, 20, 25, 30 wt.%). To achieve proper mixing, the extrusion step was repeated. Extruded composite blends were injection moulded to obtain tensile, flexural and impact test specimens. The composite's physical and mechanical properties were investigated and compared with those of neat PP and PE. Microstructural properties of $CaCO_3$ particles were investigated with X-Ray Diffraction (XRD) and Scanning Electron Microscopy (SEM) techniques. Thermal behavior of polypropylene and polyethylene were analyzed by means of differential scanning calorimetry (DSC) and thermogravimetric analysis (TGA).

XRD analysis showed that both uncoated and coated $CaCO_3$ particles had same sharp peaks at same values. Some aggregates were observed from the SEM analysis of the uncoated particles. Thermal characterization results revealed that melting point of PP was higher than that of PE, however crystallization temperature of PE was higher than PE. The onset decomposition temperature of neat PP was lower value than of neat PE. Crystallization temperature was increased with addition filler into the PP matrix. There was no change in melting temperature because it is depended on the material characteristics of polymer materials.

Tensile test results showed that yielding behavior was observed for all specimens. Brittle fracrure was observed in high calcite content specimens and transformation from ductile to brittle was observed with the addition of calcite filler. The filler content did not have a significant effect on the yield strength of composites. The filler content had a positive effect on elastic modulus of $CaCO_3$/PP and $CaCO_3$/PE composites. The Elastic modulus of composite specimens reinforced with coated calcite were higher than those of specimens reinforced with uncoated calcite. The elastic

modulus took its maximum value when the filler content was 30 wt.% for both uncoated and coated calcite. From the analytical calculations, the experimental moduli of the nanocomposites agreed well with the law of mixtures up till a filler content of 15 wt.%.

Flexural test results showed that, the values of flexural modulus and strength increases with the increase of $CaCO_3$ content. The flexural modulus and strength values of specimens with uncoated filler were higher than those of specimens with coated filler. The addition of the calcite had a negative effect on the impact strength of neat PP and PE. The impact strength values of neat PP were higher than those of the $CaCO_3$ /PP composite specimens.

REFERENCES

[1] Miracle D. B. and Donaldson S. L. (2001), Introduction to Composites, ASM Handbook vol.21, pp. 3-17.

[2]http://nptel.ac.in/courses/Webcoursecontents/IIScBANG/Composite%20Materials/pdf/Teacher_Slides/mod1.pdf

[3]http://www.essentialchemicalindustry.org/materials-andapplications/composites.html

[4] http://ed.iitm.ac.in/~shankar_sj/Courses/ED5312/Materials_for_Automobiles17.pdf

[5] http://www-old.me.gatech.edu/jonathan.colton/me4793/thermoplastchap.pdf

[6] Yilmaz G. (2008), Effects of titanate coupling agents on low density polyethylene and polypropylene blends and composites, MSc Thesis, Middle East Technical University (METU), Ankara, Turkey.

[7] Baker A.M.M. and Mead. J. (2000), Thermoplastics, in Modern Plastics Handbook, McGraw-Hill, Inc.

[8]http://www.chemaxon.com/blog/challenges-of-polymer-informatics-and-the-driving-force/

[9] Mark H. F. (2004), Encyclopedia of Polymer Science and Technology, John Wiley & Sons, Inc, Vol.2, pp. 307-328.

[10] Samsudin M. S. F. (2008), Rheological Behavior of Talc and Calcium Carbonate Filled Polypropylene Hybrid Composites, MSc. Thesis, Universiti Sains Malaysia.

[11]http://www.specialchem4polymers.com/common/shared/solutions/popup.aspx?t=1059&id=light-weight-parts

[12] ASTM D1566, Standard Terminology Relating to Rubber, ASTM International: West Conshohocken, PA.

[13] Bazherov S. (2011), Metal, ceramic and polymeric composites for various uses, Dr. John Cuppoletti (Ed.), ISBN: 978-953-307-353-8.

[14] Biron M. (2007), Thermoplastics and Thermoplastic Composites: Technical Information for Plastics Users, Elsevier, pp.11.

[15] Moritomi S., Watanabe T., Kanzaki S. (2010), Polypropylene Compounds for Automotive Applications, R&D Report, Vol. 1, pp. 1-16.

[16] Biswas J. (2005), Effects of Calcite and Zeolite on the Matrices of Polypropylene Copolymer Derivative Composites, MSc. Thesis, Inha University.

[17] Whelan T. (1994), Polymer Technology Dictionary, Chapman&Hall, London.

[18] Chan C.M., Wu J., Li J.X., Cheung Y.K., (2002), Polypropylene/calcium carbonate nanocomposites, Polymer, Vol. 43, pp. 2981-2992

[19] Zuiderduin W.C.J., Westzaan C., Hue´tink J., Gaymans R.J. (2003),Toughening of polypropylene with calcium carbonate particles, Polymer, Vol. 44, pp. 261-275

[20] G. Wang, X.Y. Chen, R. Huang, and L. Zhang, (2002), Journal of Materials Science Letters, Vol. 21, pp.985.

[21] Supaphol P., Harnsiri W., Jirawut J., (2004), Effects of calcium carbınate and its purity on crystallization and melting behavior,mechanical properties, and processability of sydiotactic polypropylene, Journal of Applied Polymer Science, Vol. 92, pp. 201-212

[22] Yang K., Yang Q., Li G., Sun Y., Feng D., (2006), Morphology and mechanical properties of polypropylene/calcium carbonate nanocomposites, Materials Letters, Vol. 60, pp. 805-809.

[23] Hanim H., Zarina R., Fuad A., Ishak M. Z. A. ,Hassan A., (2008), The Effect of calcium carbonate nanofiller on the mechanical properties and crystallization behaviour of polypropylene, Malaysian Polymer Journal, Vol. 3, pp. 38-49.

[24] Eiras D., Pessan L. A., (2009), Mechanical properties of polypropylene/calcium carbonate nanocomposites, Materials Research, Vol. 12, pp. 517-522.

[25] Lam T. D., Hoang T. V., Quang D. T., Kim J. S., (2009), Effect of nanosized and surface-modified precipitated calcium carbonate on properties of $CaCO_3$/polypropylene nanocomposites, Materials Science and Engineering, Vol. 501, pp. 87-93.

[26] Ihueze C.C. and Mgbemena C.O., (2010), Effects of reinforcement combinations of calcium carbonate nanofiller on the mechanical and creep properties of polypropylene, Journal of Minerals & Materials Characterization & Engineering, Vol. 9, pp.887-906.

[27] Lin Y., Chen H., Chan C. M., Wu J., (2010), The toughening mechanism of polypropylene/calcium carbonate nanocomposites, Polymer, Vol. 51, pp. 3277-3284.

[28] Zhang J., Han B., Zhou N.L., Fang J., Ma Z., Mo H., Shen J., (2011), Preparation and characterization of nano/micro-calcium carbonate particles/polypropylene composites, Journal of Applied Polymer Science, Vol. 119, pp. 3560-3565.

[29] Buasri A, Chaiyut N, Borvornchettanuwat K, Chantanachai N. and Thonglor K. (2012), Thermal and mechanical properties of modified $CaCO_3$/PP nanocomposites, World Academy of Science, Engineering & Technology; Issue 68, pp. 842.

[30] Zaman H.U., Hun P. D.,Khan R. A., Yoon K. B., (2012), Effect of surface-modified nanoparticles on the mechanical properties and crystallization behavior of PP/$CaCO_3$ nanocomposites, Journal of Thermoplastic Composite Materials, Vol. 26, pp. 1057-1070.

[31] Zaman H. U., Beg M., (2014), Mechanical, thermal, and morphological properties of nano-calcium carbonate/polypropylene composites modified by methacrylic acid, Journal of Thermoplastic Composite Materials, in-press.

[32] Kwon S., Kim K. J., Kim H., Kundu P. P., Kim T. J., Lee Y. K., Lee B. H., Choe S., (2002), Tensile property and interfacial dewetting in the calcite filled HDPE, LDPE, and LLDPE composites, Polymer, Vol. 43, pp. 6901-6909.

[33] Kundu P., Biswas J., Kim H., Shim S.E., Choe S., Lee D.S., (2004), Effect of calcite and calcite/zeolite hybrid fillers on LLDPE and PP composites, Vol. 23, Issue 3, pp. 230–238.

[34] Misra R. D. K., Nerikar P., Bertrand K., Murphy D., (2004), Some aspects of surface deformation and fracture of 5-20% calcium carbonate-reinforced polyethylene composites, Materials Science and Engineering, Vol. 384, pp. 284-298.

[35] Deshmane C., Yuan Q., Misra R. D. K., (2007), On the fracture characteristics of impact tested high density polyethylene-calcium carbonate nanocomposites, Materials Science and Engineering, Vol. 452-453, pp. 592-601.

[36] Schrauwen B. A. G., Govaert L. E. , Meijer H. E. H.

[37] Elleithy R. H., Ali I., Ali M. A., Zahrani S. M. , (2010), High density polythylene/micro calcium carbonate composites: a study of the morphological, thermal, and viscoelastic properties, Journal of Applied Polymer Science, Vol. 117, pp. 2413-2421.

[38] Xanthos M. (2005), Functional fillers for plastics, Wiley-Vch Verlag GmbH & Co. KgaA, Weinheim.

[39] http://www.theadvancedteam.com/laser_extruder.php

[40] Rosato D. V. (1998), Extruding Plastics, Chapman & Hall, London.

[41] http://www.plastics.com/extrusion-whatis-pg2.html

[42] Kutz M. (2011), Applied Plastics Engineering Handbook, Elsevier.

[43]http://www.custompartnet.com/wu/images/im/injectionMolding_machine_injection.png

[44] http://www.metu.edu.tr/~rgurbuz/Courses/MetE206.pdf

[45] http://mee-inc.com/hamm.html

[46] Boresi A.P. and Chong K.P. (2000), Elasticity in Engineering Mechanics , 2nd Edition, John Wiley & Sons.

[47] Koutsos V. Tensile Testing of Polymers: Lab report, University of Edinburgh.

[48] ISO-178 standard (2001), Determination of flexural properties.

[49]http://hardiepolymers.wordpress.com/2013/06/07/do-izod-and-charpy-make-the-appropriate-impact/

[50] ISO-179 standard (2001), Determination of Charpy impact properties.